Reversible Brain Creatine Deficiency in Two Sisters with Normal Blood Creatine Level

Maria Cristina Bianchi, MD,* Michela Tosetti, PhD,† Francesco Fornai, MD,‡ Maria Grazia Alessandri', PhD,† Paola Cipriani, MD,† Giuseppe De Vito, MD,† and Raffaello Canapicchi, MD*†

We describe a new creatine metabolism disorder in 2 young sisters who suffered from mental retardation and severe language delay. Blood examination, investigation of the most common neurometabolic disorders, and brain magnetic resonance imaging were normal. Diagnosis was established only by means of in vivo proton magnetic resonance spectroscopy, which disclosed generalized depletion of creatine in the brain. Creatine monohydrate oral administration led to almost complete brain creatine level restoration along with improvement of the patients' disabilities.

Bianchi MC, Tosetti M, Fornai F, Alessandri' MG, Cipriani P, De Vito G, Canapicchi R. Reversible brain creatine deficiency in two sisters with normal blood creatine level. Ann Neurol 2000;47:511–513

Creatine (Cr), and its phosphorylated form phosphocreatine (PCr), provide a fast available substrate for energy metabolism of muscles and the central nervous system.[1] Despite the importance of Cr, its metabolism and distribution in humans are not well understood. Recently, a new inborn error of metabolism was identified that is the result of guanidinoacetate methyltransferase (GAMT) deficiency and that manifests as systemic Cr depletion and is shown by an abnormal brain magnetic resonance imaging (MRI) scan.[2–6]

In this study, we report a novel brain Cr deficiency syndrome disclosed by means of brain proton magnetic resonance spectroscopy (^{1}H MRS). Unlike the GAMT deficiency cases, our patients had normal peripheral Cr and guanidoacetic acid (GAA) concentrations and a distinct clinical phenotype.

From the *Neuroradiology Department, S Chiara Hospital, †Stella Maris Scientific Institute, and ‡Department of Human Morphology and Applied Biology, University of Pisa, Pisa, Italy.

Received Aug 5, 1999, and in revised form Nov 9. Accepted for publication Nov 11, 1999.

Address correspondence to Dr Bianchi, Neuroradiology Department, S Chiara Hospital, Via Roma 67, Pisa 56100, Italy.

Patients and Methods

Two sisters (BV and BA), 4 years 4 months and 6 years 5 months old, respectively, were referred to our hospital because of mental retardation and severe language delay. Neurological examination did not show any focal symptom.

The girls were born to healthy unrelated Italian parents after uncomplicated pregnancy and delivery. They started walking unaided at 24 months and started speaking the first words at 30 months. The younger sister had a febrile seizure at 18 months. Routine blood and urine analysis and extensive investigation for neurometabolic disorders (including screening for mitochondrial disorders and metabolic screening of a 24-hour sample of urine with assessment of amino acids, organic acids, oligosaccharides, and mucopolysaccharides) were normal. Despite these preliminary results, the girls underwent conventional MRI and ^{1}H MRS scanning of the brain, following our standard clinical protocol.

Magnetic resonance (MR) studies were performed in the same setting, using a 1.5-T clinical MR scanner (Advantage Signa 1.5; GE, Milwaukee, WI), as described previously.[7] Localized MR spectra were determined by using a single-voxel short echo time (TE) stimulated echo acquisition mode technique (STEAM; repetition time [TR] = 2,010 mec; TE = 30 msec; mixing time = 13.7 msec; 256 scans; volume of interest dimension = 3.4 ml). Spectra were processed[8] off-line with the Spectral Analysis GE/Interactive Data Language (SAGE/IDL), and evaluation of metabolites concentration was performed by using a method similar to that described by Ernst and co-workers.[9,10]

MRI was normal, but ^{1}H MRS revealed the total absence of the Cr/PCr peak in the paraventricular white matter, in the cerebellum, and in the parieto-occipital cortex (Fig 1). The Cr biosynthetic pathway was therefore investigated.

Blood concentrations of Cr and GAA turned out to be within normal values, thus excluding a systemic Cr synthesis deficit (serum Cr: in BV and BA, 122 and 95 μmol/L, respectively; normal, 10–200 μmol/L; serum guanidinoacetate: in BV and BA, 0.3 and 0.5 μmol/L, respectively; normal, 0.4–3.0 μmol/L). Therapy was first attempted with oral administration of L-arginine (300 mg/kg/day) to rule out a possible deficit of the first biochemical step of endogenous Cr synthesis (ie, arginine:glycine amidinotransferase). Because ^{1}H MRS revealed no Cr increase after 2 months of L-arginine treatment, oral Cr monohydrate was subsequently started at a dose of 400 mg/kg/day. The effects of treatment were monitored by consecutive ^{1}H MRS scanning performed after 3, 9, and 16 months of continuous Cr intake. After 3 months of therapy, brain Cr concentration reached 40% of normal value, and after 9 months it reached 80%. At this time, blood Cr had increased to 344 μmol/L in BA and 328 μmol/L in BV. After 16 months, brain Cr was restored to normal in the gray matter and cerebellum, but it was still slightly less than the normal value in the hemispheric white matter (Fig 2).

Nonverbal intelligence, visual–perceptual abilities, and fine motor skills were rated before and during therapy. For this purpose, we applied the performance and the eye–hand coordination subscales of the Griffiths Developmental Scales in the younger sister (BV),[11,12] and we used the Leiter In-

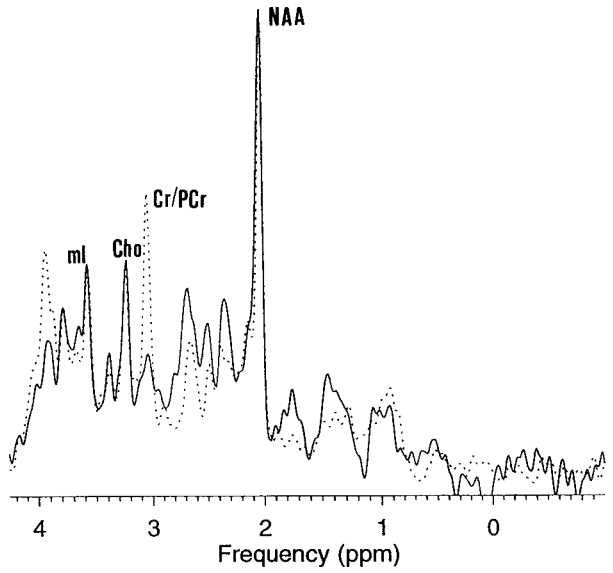

Fig 1. Overlapped in vivo proton magnetic resonance spectra of the parieto-occipital cortex in a patient with brain creatine deficiency. The solid tracing *spectrum was determined before treatment; the* dotted tracing *spectrum was determined after 9 months of oral treatment with creatine. Resonance assignments are the result of* N*-acetylaspartate (NAA; at 2.01 ppm), creatine and creatine phosphate (Cr/PCr; at 3.05 ppm), choline-containing compounds (Cho; at 3.20 ppm), and myoinositol (mI; at 3.56 ppm).*

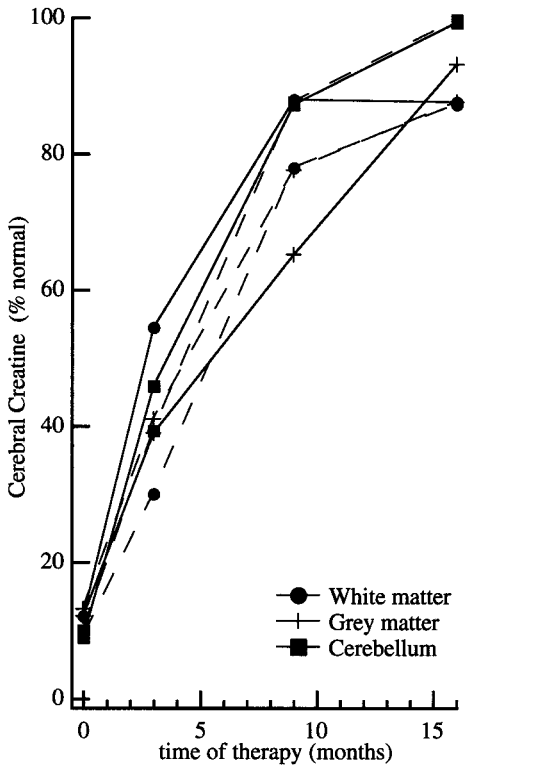

Fig 2. Time course of brain creatine restoration (as percentage of normal concentrations in young healthy adult controls) detected by proton magnetic resonance spectroscopy in 2 sisters with brain creatine deficiency (dotted tracing = *Patient BA;* solid tracing = *Patient BV*). *The graph refers to a 16-month period of therapy with oral creatine administration at a dose of 400 mg/kg/day.*

ternational Performance Scale (LIPS)[13] and the Visual Motor Integration Test (VMI)[14] with the older sister.

Before starting therapy, BV was 4 years 4 months old and had a performance score of 42 and an eye–hand coordination score of 57, as measured by using the Griffiths Developmental Scales. After 16 months of therapy, the scores increased to 68 and 62, respectively, thus demonstrating an acceleration of the rate of cognitive development (corresponding to 20 months of progress in 16 months). It was only feasible to assess BV's visual–perceptual abilities after 16 months of Cr supplementation, because at the time of the first evaluation she was not even able to copy the simplest figures of the VMI. At this time, she received a standard score of 77, which was in the borderline range for her chronological age. Language abilities also improved but at a slower rate, compared with nonverbal skills, and were discrepant with respect to mental age expectation.

At the time of the first observation, BA was 6 years 5 months old and she achieved an LIPS IQ score of 65 and a VMI standard score of 60. After 16 months of therapy, her LIPS IQ score was almost unchanged, but the VMI standard score had increased to 77. Therefore, in a similar manner as her sister, she made an unusually rapid progress in the acquisition of visual perceptual and fine motor skills, whereas the rate of general cognitive development, as assessed by LIPS, was slow.

Concerning language outcome, a constant lag in the acquisition of different language skills was observed, when assessed by standardized tests of productive and receptive vocabulary and grammar. However, analysis of spontaneous speech (ie, free conversation with parents and/or peers, and play situations) revealed a marked improvement in communicative intent, together with a better capacity to correctly follow simple verbal commands and a more adequate use of language, because she expressed herself in a coherent and intelligible way. She also demonstrated better socioemotional behavior, with improvement of attention span, mood control, and social skills.

Discussion

The first report of an inborn error of Cr metabolism was described by Stockler and associates[2] in a 22-month-old boy with progressive muscular hypotonia and extrapyramidal symptoms. The baby had systemic depletion of Cr and extremely low excretion of creatinine. A brain MRI scan revealed signal abnormalities in the globus pallidus, and ^{1}H MRS scanning showed the absence of brain Cr and high concentrations of guanidinoacetate, both in plasma and in the brain. Clinical symptoms and biochemical abnormalities improved after oral treatment with Cr monohydrate. On the basis of these observations, an enzyme defect in Cr

biosynthesis was first hypothesized and subsequently proved at the level of GAMT activity, in the liver of the patient.[3] The authors also identified the mutation in the GAMT alleles of this patient, which established the genetic nature of the disorder.[4] Two additional cases were subsequently identified by Schulze and associates[5] and by Ganesan and colleagues[6] in a 4-year-old girl and in a 5-year-old boy. Both had the same biochemical and brain spectroscopic abnormalities, and, clinically, they presented the same movement disorder described previously, with dyskinesia and dystonias in addition to tonic seizures that were resistant to antiepileptic drugs. A brain MRI scan confirmed the abnormalities in the globus pallidus and also showed a diffuse signal alteration in the hemispheric white matter.

In the present report, we describe 2 cases of a new error of Cr metabolism characterized by different clinical and biochemical features. In fact, differently from the patients previously reported, the 2 sisters only suffered from mild mental retardation and severe language delay, whereas their blood concentrations of Cr and GAA and brain MRI scans were normal. In other words, the Cr deficiency was only confined to the brain. Because Cr synthesis is currently believed to occur only in the liver and pancreas,[1] it is likely that the 2 sisters suffer from a specific dysfunction of the central nervous system Cr transporter. Nonetheless, as in the GAMT deficit cases, oral administration of Cr monohydrate restored the Cr concentration of the brain and led to obvious clinical improvement.

Biosynthesis and physiological functions of Cr have been addressed, but still little is known about brain Cr uptake and brain Cr distribution.[15,16] Brain Cr contents of our patients increased linearly to 80% of the normal values during the first 9 months of therapy. In contrast, the patient with GAMT deficiency reached the same amount of brain Cr during a longer period of therapy and with a biphasic trend—a fast phase (in the first 3 months) and a slower phase (in the following 22 months).[3] In our cases, it might be assumed that the Cr transporter function has been forced by markedly increasing blood Cr concentration, which thus indicates hypofunction of the transporter protein complex.

In conclusion, these data suggest the existence of a new Cr metabolism disorder that might be caused by either defective Cr brain transport or other unknown defects. Because blood tests were normal in these patients, ^{1}H MRS scanning proved to be the only diagnostic tool and the only means to monitor the efficacy of treatment.

This disorder is treatable; therefore, its early diagnosis might be critical, to prevent irreversible brain damage. It must be considered in the differential diagnosis of the broad range of unexplained neuropsychiatric disorders in children and it can be ruled out only by using in vivo ^{1}H MRS, which, at present, is available in many clinical MR systems and is easy to perform.

We thank Professors F. Hanefeld and D. H. Hunneman for their valuable suggestions and for the creatine and the guanidoacetic acid assay.

References

1. Walker JB. Creatine: biosynthesis, regulation, and function. Adv Enzymol Relat Areas Mol Biol 1979;50:177–242
2. Stockler S, Holzbach U, Hanefeld F, et al. Creatine deficiency in the brain: a new, treatable inborn error of metabolism. Pediatr Res 1994;36:409–413
3. Stockler S, Hanefeld F, Frahm J. Creatine replacement therapy in guanidinoacetate methyltransferase deficiency, a novel inborn error of metabolism. Lancet 1996;348:789–790
4. Stockler S, Isbrandt D, Hanefeld F, et al. Guanidinoacetate methyltransferase deficiency: the first inborn error of creatine metabolism in man. Am J Hum Genet 1996;58:914–922
5. Schulze A, Hess T, Wevers R, et al. Creatine deficiency syndrome caused by guanidinoacetate methyltransferase deficiency: diagnostic tools for a new inborn error of metabolism. J Pediatr 1997;131:626–631
6. Ganesan V, Johnson A, Connelly A, et al. Guanidinoacetate methyltransferase deficiency: new clinical features. Pediatr Neurol 1997;17:155–157
7. Mascalchi M, Tosetti M, Plasmati R, et al. Proton magnetic resonance spectroscopy in an Italian family with spinocerebellar ataxia type 1. Ann Neurol 1998:43:244–252
8. Kreis R, Farrow N, Ross BD. Localized ^{1}H NMR spectroscopy in patients with chronic hepatic encephalopathy: analysis of changes in cerebral glutamine, choline and inositols. NMR Biomed 1991;4:109–116
9. Ernst T, Kreis R, Ross BD. Absolute quantitation of water and metabolites in the human brain. I. Compartments and water. J Magn Reson 1993;102:1–8
10. Ernst T, Kreis R, Ross BD. Absolute quantitation of water and metabolites in the human brain. II. Metabolite concentrations. J Magn Reson 1993;102:9–19
11. Griffiths R. The abilities of babies: a study in mental measurement. Oxon, UK: Test Agency, 1986
12. Griffiths R. The abilities of young children: a comprehensive system of mental measurement for the first eight years of life. Oxon, UK: Test Agency, 1984
13. Levine MN. Leiter International Performance Scale: a handbook. Los Angeles: Western Psychological Services, 1982
14. Beery KE. The Developmental Test of Visual-Motor Integration, Revised. Cleveland: Modern Curriculum Press, 1989
15. Moller A, Hamprecht B. Creatine transport in cultured cells of rat and mouse brain. J Neurochem 1989;52:544–550
16. Sora I, Richman J, Santoro G, et al. The cloning and expression of a human creatine transporter. Biochem Biophys Res Commun 1994;204:419–427

Sonic Hedgehog Signal Peptide Mutation in a Patient with Holoprosencephaly

Mitsuhiro Kato, MD,* Eiji Nanba, MD,†
Shinjiro Akaboshi, MD,‡ Takashi Shiihara, MD,‡
Aiko Ito, MD,* Tomomi Honma, MD,*
Kenji Tsuburaya, MD,§ and Kiyoshi Hayasaka, MD*

We investigated the molecular basis of holoprosencephaly in a sporadic patient and identified a novel missense mutation in the signal sequence of the sonic hedgehog (Shh) gene. Magnetic resonance imaging of the head showed a lobar type of holoprosencephaly and partial agenesis of the anterior corpus callosum. He was treated for craniosynostosis at 7 months of age. All three exons of the Shh gene were amplified by polymerase chain reaction from genomic DNA of the patient and controls. Sequencing analysis of the polymerase chain reaction fragments, screened by single-strand conformation polymorphism analysis, revealed a heterozygous mutation of a T-to-C substitution at nucleotide position 50. This mutation predicted an amino acid replacement of leucine to proline at codon 17 located in the signal peptide of SHH protein. It probably disturbs the translocation of the protein into the endoplasmic reticulum and may lead to holoprosencephaly because of haploinsufficiency of Shh.

Kato M, Nanba E, Akaboshi S, Shiihara T, Ito A, Honma T, Tsuburaya K, Hayasaka K. Sonic hedgehog signal peptide mutation in a patient with holoprosencephaly. Ann Neurol 2000;47:514–516

Holoprosencephaly is a brain malformation caused by impaired midline cleavage of the embryonic forebrain.[1] It can be graded according to the degree of severity as alobar, semilobar, or lobar holoprosencephaly.[1] Various degrees of facial dysmorphism are associated with this disorder, graded from hypotelorism or single maxillary central incisor to cyclopia, single median eye. The incidence of holoprosencephaly was estimated as 0.4% among induced abortions.[2] It is usually sporadic and occasionally associated with numerous chromosomal abnormalities, especially with trisomy 13, and in most cases the cause is unknown.[3] Cytogenetic analysis defined as many as 12 loci implicated in the pathogenesis of holoprosencephaly.[4] The sonic hedgehog (Shh) gene on chromosome 7q36 has been identified as a gene responsible for holoprosencephaly in humans.[5,6] The Shh gene consists of three exons spanning about 15 kb, encoding a polypeptide of 462 amino acids. The SHH protein is a secreted protein that is transported to the endoplasmic reticulum and cleaved of its signal peptide. Then, it undergoes autoproteolytic cleavage into a 19-kd amino-terminal product (SHH-N) and a carboxy-terminal product of 25-kd (SHH-C) in the endoplasmic reticulum.[7] To date, 9 of 42 families with familial autosomal dominant holoprosencephaly have been reported to have Shh gene mutations. In contrast, only 1 of 184 sporadic cases of holoprosencephaly was attributable to Shh gene mutation.[4] All mutations previously reported are distributed in the SHH-N and SHH-C domain, and none have been found in the sequence of the signal peptide.

Here, we report a novel mutation in the signal peptide of the Shh gene in a sporadic case of holoprosencephaly with anterior callosal agenesis.

Subjects and Methods

Case Report

The patient was the first child of unrelated healthy parents. His mother caught a common cold at the fifth month of gestation. He was born at term by cesarean section because of premature rupture of the membranes and velamentous insertion. Birth weight was 2,680 g, length was 44.8 cm (−2.7 SD), and head circumference was 29.5 cm (−2.9 SD). He was nursed in an incubator for 1 week because of respiratory disturbance and poor sucking. He had a septonasal recess and peculiar face at birth. At 1 month of age, he showed three generalized tonic-clonic convulsions with fever. He underwent craniotomy with early closure of cranial sutures at 7 months of age. He showed severe psychomotor delay, however, but no regression. He has been institutionalized since 3 years of age.

At the age of 19 years, he showed small stature (body height, 121 cm [−8.8 SD]; body weight, 14.8 kg), microcephaly (head circumference, 43.2 cm [−9.8 SD]), and low-grade body temperature (mean, 34.0°C). He had many minor anomalies (hypotelorism, low nasal bridge, hypoplasia of nasal septum, macroglossia, micropenis, and cryptorchidism) and joint contractures at knees and ankles. Neurological examination disclosed severe psychomotor developmental delay as follows: no walking, no speech, and no response to spoken commands. There were no abnormal laboratory findings in the biochemical analysis, including liver and renal functions and serum electrolytes. Chromosomal analysis was 46, XY. Electroencephalogram revealed no paroxysmal activity. Brainstem auditory-evoked potential and short latency somatosensory-evoked potential were normal. Cranial

From the *Department of Pediatrics, Yamagata University School of Medicine, Yamagata; †Gene Research Center, and ‡Division of Child Neurology, Institute of Neurological Sciences, Faculty of Medicine, Tottori University, Yonago, Tottori; and §Department of Neurology, National Sanatorium Yonezawa Hospital, Yonezawa, Yamagata, Japan.

Received Sep 14, 1999, and in revised form Nov 12. Accepted for publication Nov 12, 1999.

Address correspondence to Dr Kato, Department of Pediatrics, Yamagata University School of Medicine, Iida-nishi 2-2-2, Yamagata 990-9585, Japan.

computed tomography showed mild dilatation of the posterior part of the lateral ventricles, or colpocephaly. A cranial magnetic resonance imaging scan revealed partial agenesis of the anterior part of the corpus callosum and fusion of the frontal lobes and basal ganglia across the midline, which indicates holoprosencephaly (Fig 1). Focal pachygyria was seen in the lateral part of the temporal lobes. Both the genu and the splenium of the corpus callosum appeared to be truncated.

Fig 1. T2-weighted axial (A) and sagittal (B) magnetic resonance imaging scans of the patient. Anteroinferior part of the bilateral basal ganglia fused across the midline. Only a deformed body and splenium of the corpus callosum were observed (arrowheads). *The anterior part of the corpus callosum was absent. Part of temporal lobes showed wide gyri and increased thickness of the cortex* (arrows), *which implied cortical dysplasia.*

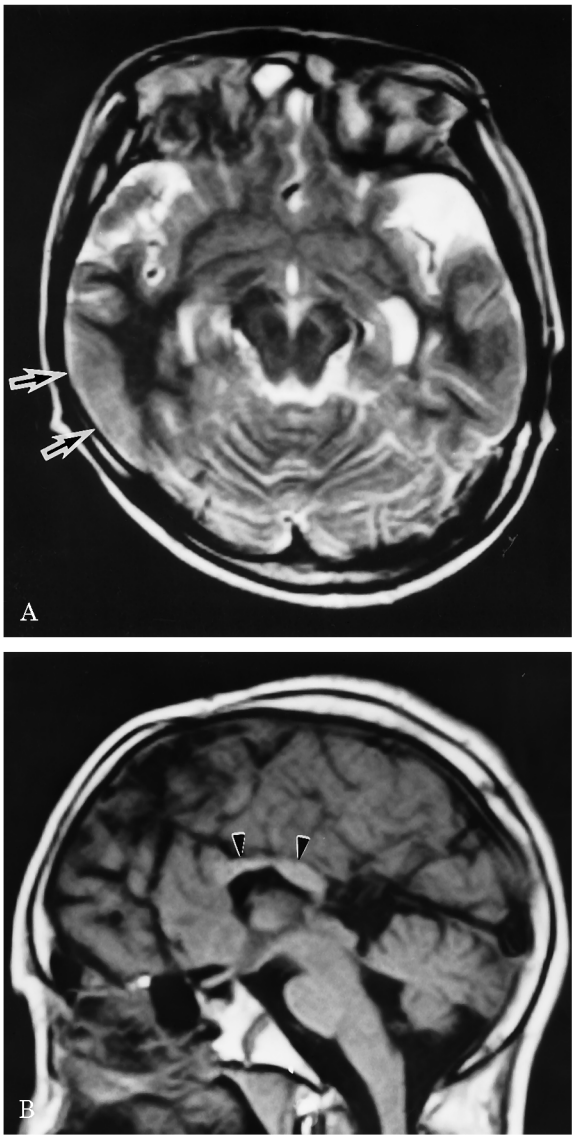

Analysis of the Shh gene

Genomic DNA was extracted from peripheral blood leukocytes by the standard method.

All coding regions of the Shh gene (exons 1 to 3) were amplified by polymerase chain reaction (PCR), using sets of primers previously reported,[5,8] and used for single-strand conformational polymorphism (SSCP) analysis. Exons 2 and 3 were amplified as two and three fragments, respectively.

The denatured PCR products were electrophoresed on a 12% polyacrylamide gel at room temperature (22°C) or at 4°C by the reported method.[9]

The PCR products were purified by using a QIAquick PCR Purification Kit (Qiagen, Hilden, Germany) and were directly sequenced by using a BigDye Terminator Cycle Sequencing FS Ready Reaction Kit (ABI) on an ABI Prism 310 Genetic Analyzer (PE Applied Biosystems, Foster City, CA).

Results

The fragment including exon 1 showed an aberrant SSCP pattern at room temperature (data not shown). DNA sequence analysis revealed that the patient was heterozygous for a T-to-C substitution at nucleotide 50 of the Shh gene (Fig 2). This mutation predicted replacement of a leucine residue with proline at codon 17 in the signal peptide. None of the detected SSCP alterations were found in 100 normal chromosomes of unrelated healthy Japanese controls.

Discussion

Holoprosencephaly has a diversity of clinical expression and a wide variety of associated brain malformations. Clinical variety has also been observed among the affected members of the same family. Studies of familial cases have indicated that there is no genotype–phenotype correlation between the type of mutation and its location in the Shh gene.[10] Genotype–phenotype correlation in the isolated cases, or the phenotype of the case reported here carrying the mutation in the signal peptide, are still unclear. The factors that modulate the clinical severity remain to be clarified.[10]

Fig 2. Nucleotide sequence of the sonic hedgehog gene from the patient. A heterozygous T-to-C transversion at position 50, which results in an amino acid change of leucine (CTG) to proline (CCG), was shown.

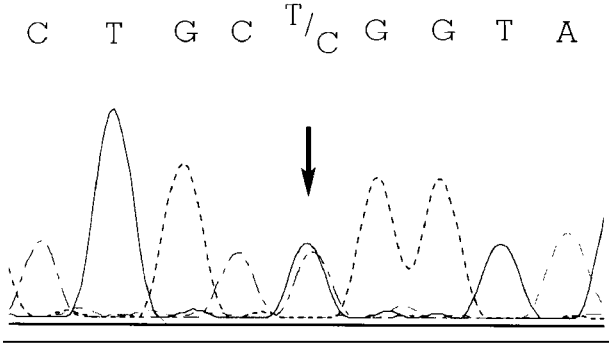

In this study, we showed that the patient had a heterozygous mutation in the sequence of the signal peptide of the Shh gene. Signal peptides have three domains, ie, an amino-terminal positively charged region, a central, hydrophobic part (h-region), and a more polar carboxy-terminal domain.[11] The h-region, which consists of strings of leucine residues, is critical for translocation.[11] The amino acid replacement of leucine with proline, in the h-region in our case, did not markedly change its hydrophobicity but influenced formation of the beta structure of the peptide. It probably disturbs the translocation of the protein into the endoplasmic reticulum and may lead to holoprosencephaly because of haploinsufficiency of Shh.

Our case showed partial agenesis of the anterior portion of the corpus callosum. Agenesis of the corpus callosum is frequently associated with multiple pathogenetic factors. In partial agenesis, the posterior part is usually missing because the corpus callosum develops in an anteroposterior manner. However, anterior agenesis can occur with a mild type of holoprosencephaly.[12] The SHH protein induces ventral neurons in the forebrain,[13] and holoprosencephaly lacks the division of hemispheres, especially in the anterior part of the forebrain. There have been few studies of the Shh gene mutation related to the associated brain anomalies. Our case suggested that the signal peptide mutation of the Shh gene may result in a milder type of holoprosencephaly. Further investigation is required to clarify the factors affecting the severity of holoprosencephaly.

This study was supported in part by grants from the Ministry of Education, Science and Culture and by Grants for Pediatric Research and for Nervous and Mental Disorders from the Ministry of Health and Welfare, Japan.

We thank Dr Mitsuo Oshimura, Department of Molecular and Cell Genetics, School of Life Sciences, Faculty of Medicine, Tottori University, for sequencing.

References

1. Cohen MM Jr, Sulik KK. Perspectives on holoprosencephaly: part II. Central nervous system, craniofacial anatomy, syndrome commentary, diagnostic approach, and experimental studies. J Craniofac Genet Dev Biol 1992;12:196–244
2. Matsunaga E, Shiota K. Holoprosencephaly in human embryos: epidemiologic studies of 150 cases. Teratology 1977;16:261–272
3. Leech RW, Shuman RM. Holoprosencephaly and related midline cerebral anomalies: a review. J Child Neurol 1986;1:3–18
4. Roessler E, Muenke M. Holoprosencephaly: a paradigm for the complex genetics of brain development. J Inherit Metab Dis 1998;21:481–497
5. Roessler E, Belloni E, Gaudenz K, et al. Mutations in the human sonic hedgehog gene cause holoprosencephaly. Nat Genet 1996;14:357–360
6. Belloni E, Muenke M, Roessler E, et al. Identification of sonic hedgehog as a candidate gene responsible for holoprosencephaly. Nat Genet 1996;14:353–356
7. Lee JJ, Ekker SC, von Kessler DP, et al. Autoproteolysis in hedgehog protein biogenesis. Science 1994;266:1528–1537
8. Roessler E, Belloni E, Gaudenz K, et al. Mutations in the C-terminal domain of sonic hedgehog cause holoprosencephaly. Hum Mol Genet 1997;6:1847–1853
9. Yuasa I, Umetsu K, Vogt U, et al. Human orosomucoid polymorphism: molecular basis of the three common ORM1 alleles, ORM1*F1, ORM1*F2, and ORM1*S. Hum Genet 1997;99:393–398
10. Ming JE, Roessler E, Muenke M. Human developmental disorders and the sonic hedgehog pathway. Mol Med Today 1998;4:343–349
11. von Heijne G. The signal peptide. J Membr Biol 1990;115:195–201
12. Rubinstein D, Cajade-Law AG, Youngman V, et al. The development of the corpus callosum in semilobar and lobar holoprosencephaly. Pediatr Radiol 1996;26:839–844
13. Ericson J, Muhr J, Placzek M, et al. Sonic hedgehog induces the differentiation of ventral forebrain neurons: a common signal for ventral patterning within the neural tube [published erratum appears in Cell 1995;82:following 165]. Cell 1995;81:747–756

Dopa-Responsive Dystonia due to a Large Deletion in the GTP Cyclohydrolase I Gene

Yoshiaki Furukawa, MD,* Mark Guttman, MD,† Steven P. Sparagana, MD,‡§ Joel M. Trugman, MD,‖ Keith Hyland, PhD,§¶ Philip Wyatt, MD, PhD,# Anthony E. Lang, MD,** Guy A. Rouleau, MD, PhD,†† Mitsunobu Shimadzu, PhD,‡‡ and Stephen J. Kish, PhD†

Although it is assumed that most patients with autosomal dominant dopa-responsive dystonia (DRD) have a GTP cyclohydrolase I dysfunction, conventional genomic DNA sequencing of the gene (GCH1) coding for this enzyme fails to reveal any mutations in about 40% of DRD patients, which makes molecular genetic diagnosis difficult. We found a large heterozygous GCH1 deletion, which cannot be detected by the usual genomic DNA sequence analysis, in a three-generation DRD family and conclude that a large genomic deletion in GCH1 may account for some "mutation-negative" patients with dominantly inherited DRD.

Furukawa Y, Guttman M, Sparagana SP, Trugman JM, Hyland K, Wyatt P, Lang AE, Rouleau GA, Shimadzu M, Kish SJ. Dopa-responsive dystonia due to a large deletion in the GTP cyclohydrolase I gene. Ann Neurol 2000;47:517–520

Dopa-responsive dystonia (DRD) is a syndrome dominated by childhood-onset dystonia and is characterized by a dramatic and sustained response to levodopa.[1] There are two known types of DRD, namely, autosomal dominant GTP cyclohydrolase I (GTPCH)-deficient DRD and autosomal recessive tyrosine hydroxylase–deficient DRD.[1–3] Using usual genomic DNA sequencing of the gene (GCH1) coding for GTPCH, the enzyme which catalyzes the first step in the biosynthesis of tetrahydrobiopterin (the cofactor for tyrosine hydroxylase), more than 50 different GCH1 mutations have been found in patients with DRD.[1,2,4–14] However, approximately 40% of genetically examined DRD patients have no mutations in the coding region (including the splice sites) of GCH1, although it is assumed that most patients with dominantly inherited DRD probably have a GTPCH dysfunction. Thus, the present conventional genomic DNA testing for the autosomal dominant form of DRD is not suitable for routine clinical practice. In this investigation, we sequenced the GCH1 coding region in four DRD pedigrees and identified independent mutations in three families but not in a three-generation family. To evaluate whether this "mutation-negative" family with DRD has a large deletion in GCH1 that cannot be detected by usual genomic DNA sequencing of this gene, we conducted GCH1 cDNA sequence and genomic Southern blot analyses.

Patients and Methods

DRD Pedigrees

All probands in four DRD families manifested foot dystonia during childhood and responded to relatively low doses of levodopa (Table). Family A had three generations of patients with DRD (Fig 1A). Four patients (affected members; I-1, II-2, II-4, and III-4) in this family, developed dystonia of the lower limbs between 3 and 11 years of age. Both twins (III-1 and III-2) complained of occasional manifestations of mild dystonic posture of the foot after extreme exercise in their school days, but no abnormal symptoms and signs were demonstrated on repeated neurological examinations. The study was approved by the institutional review board of the Centre for Addiction and Mental Health. All subjects gave written, informed consent.

Sequencing of Genomic DNA

Genomic DNA from peripheral leukocytes was obtained by standard extraction methods. Polymerase chain reaction (PCR) primers for amplification of GCH1 exons and the amplification conditions were the same as reported.[2,4] Amplified DNA fragments were directly sequenced.[7] A deletion in exon 6 was suspected from direct sequencing in Family C. The PCR product in this family was subcloned and sequenced as described.[5,7] In addition, an essential part (588 bp upstream) of the 5′ region and a poly(A) signal on the 3′ end of GCH1 were sequenced in the proband in Family A.[9,12]

Sequencing of cDNA

Total RNA from lymphocytes in Family A was reverse-transcribed (RT) into first-strand cDNA using random hexamer primers.[7] GCH1 cDNA was first amplified by PCR, using the exon 1 sense and exon 6 antisense primers. The target sequence was reamplified by using nested primers, 5′-

From the *Movement Disorders Research Laboratory and †Human Neurochemical Pathology Laboratory, Centre for Addiction and Mental Health, Clarke Division, #Department of Genetics, North York General Hospital, and **Movement Disorders Centre, Toronto Hospital, Toronto, Ontario; and ††Montreal General Hospital Research Institute, Montreal, Quebec, Canada; ‡Texas Scottish Rite Hospital for Children, §Department of Neurology, University of Texas Southwestern Medical Center, and ¶Institute of Metabolic Disease, Baylor University Medical Center, Dallas, TX; ‖Department of Neurology, University of Virginia School of Medicine, Charlottesville, VA; and ‡‡Department of Genetics, Mitsubishi Kagaku Bio-Clinical Laboratories, Inc, Tokyo, Japan.

Received Aug 11, 1999, and in revised form Nov 8 and Nov 16. Accepted for publication Nov 16, 1999.

Address correspondence to Dr Furukawa, Movement Disorders Research Laboratory (R 211), Centre for Addiction and Mental Health, Clarke Division, 250 College Street, Toronto, Ontario, Canada M5T 1R8.

Table. Clinical Characteristics and Mutations of the GTP Cyclohydrolase I Gene Detected by Usual Genomic DNA Sequencing in Probands of Four Families with Dopa-Responsive Dystonia

DRD Family	Age (yr)	Sex	Age at Onset (yr)	Initial Site of Dystonia	Family History	Nucleotide Change in the Coding Region	Effect on Coding Sequence
A	53	F	7	Right foot	+	No change[a]	—
B	26	F	7	Right foot	+	**G**^{166}AG → **T**AG	Nonsense mutation (Glu 56 Stop in exon 1)[b]
C	59	M	3	Feet	+	**A**^{631}**T**G (631 del AT)	Frameshift (termination in exon 6)[b]
D	28	F	12	Right foot	−	C^{553}**T**T → C**G**T	Missense mutation (Leu 185 Arg in exon 5)[c]

[a]In Family A (English-Canadian), no mutation in either the coding region or the splice sites of the GTP cyclohydrolase I gene (GCH1) was identified.
[b]Mutations in Family B (European-American) and Family C (African-American) have been found in other dopa-responsive dystonia (DRD) pedigrees previously.[7,12]
[c]A novel missense mutation in Family D (German/Irish, American Indian/French) affects a highly conserved amino acid residue.[16]

CCATGCAGTTCTTCACCAAG-3′ and 5′-TGAAGCTC-AGCTCCTAATGAG-3′ (set in exons 1 and 6). The nested RT-PCR products were subcloned and sequenced.[5,7] These products contain type 1 GCH1 mRNA but not type 2 GCH1 mRNA (an inactive isoform), because regions corresponding to the antisense primers in exon 6 are spliced out in type 2 mRNA.[6,15] No other mature GCH1 mRNAs caused by alternative splicing were detected in lymphocytes from normal subjects.[6]

Genomic Southern Blotting

After digestion with *Hind*III, genomic DNA of 10 members in Family A (all individuals shown in Fig 1A, except for II-1) and of 20 neurologically normal controls was separated in a 1% agarose gel and transblotted onto a Biodyne B nylon filter (Pall Biosupport Division, Ann Arbor, MI). The filter was hybridized with a [α-^{32}P]dCTP-labeled RT-PCR product of GCH1 (including the entire coding region) or a [α-^{32}P]dCTP-labeled PCR product of a GCH1 exon as a probe. Hybridization and washing were performed according to the manufacturer's recommendations.

Results

In Family A, we found no mutation in either the coding region or the splice sites of GCH1 by conventional genomic DNA sequencing of this gene, whereas we identified independent heterozygous mutations in the three other families (see Table).

Karyotype analysis demonstrated no abnormality in the proband of Family A. Additional genomic DNA sequencing of the essential part of the 5′ region and the poly(A) signal on the 3′ end of GCH1 in this index patient failed to reveal any mutation. However, in 6 subjects (4 affected members [I-1, II-2, II-4, and III-4] and both twins [III-1 and III-2]) in Family A, four GCH1 mRNA transcripts (the normal cDNA and three different mutant cDNAs lacking either exon 3, exons 3 and 4, or exons 3, 4, and 5) were detected by sequencing of the nested RT-PCR products (see Fig 1B). Each mutant cDNA had a predictable premature termination codon caused by a frameshift. Southern blot analysis of *Hind*III-digested genomic DNA, using the RT-PCR or exon 2–PCR product probe, revealed an aberrant band (7.8 kb) in all of the 6 subjects (Fig 2A). This abnormal band was not detected in their 2 unaffected siblings (II-3 and III-3) and 2 spouses (I-2 and II-5) and in 20 normal controls. A normal band (9.0 kb) shown by the exon 2–PCR product probe was also hybridized with the exon 3–PCR product probe (see Fig 2B), indicating that both GCH1 exons 2 and 3 are located in this normal fragment. However, the 7.8-kb aberrant band, which is derived from the 9.0-kb normal band, disappeared when the exon 3–PCR product was used as a probe. Thus, there was a large heterozygous deletion (~1.2 kb genomic deletion in GCH1, based on Southern blotting of *Hind*III-digested genomic DNA) involving exon 3 in the 6 subjects in Family A.

Discussion

To our knowledge, this is the first report of a large GCH1 deletion in DRD, which cannot be detected by usual genomic DNA sequencing of GCH1.

In previous reports on DRD, in which a relatively large number of families was examined genetically, 30 of 74 pedigrees had no mutations in the coding region (including the splicing junctions) of GCH1.[2,4,5,7–12] Because the 30 pedigrees include families having an apparently sporadic patient or only a few affected siblings,[9–12] there is a possibility that some of these families might have autosomal recessive tyrosine hydroxylase–deficient DRD.[3] However, for dominantly inherited mutation-negative pedigrees with DRD, possible explanations are the following: (1) a mutation in noncoding regulatory regions of GCH1, (2) a large deletion of GCH1, (3) an intragenic duplication or inversion of GCH1, and (4) a mutation in regulatory genes having an influence on GCH1 expression. An earlier chromosomal study failed to reveal any large-scale deletions or gene rearrangements at the DRD locus on chromosome 14q.[17] Although the essential part of the 5′ region was sequenced in 10 DRD families,

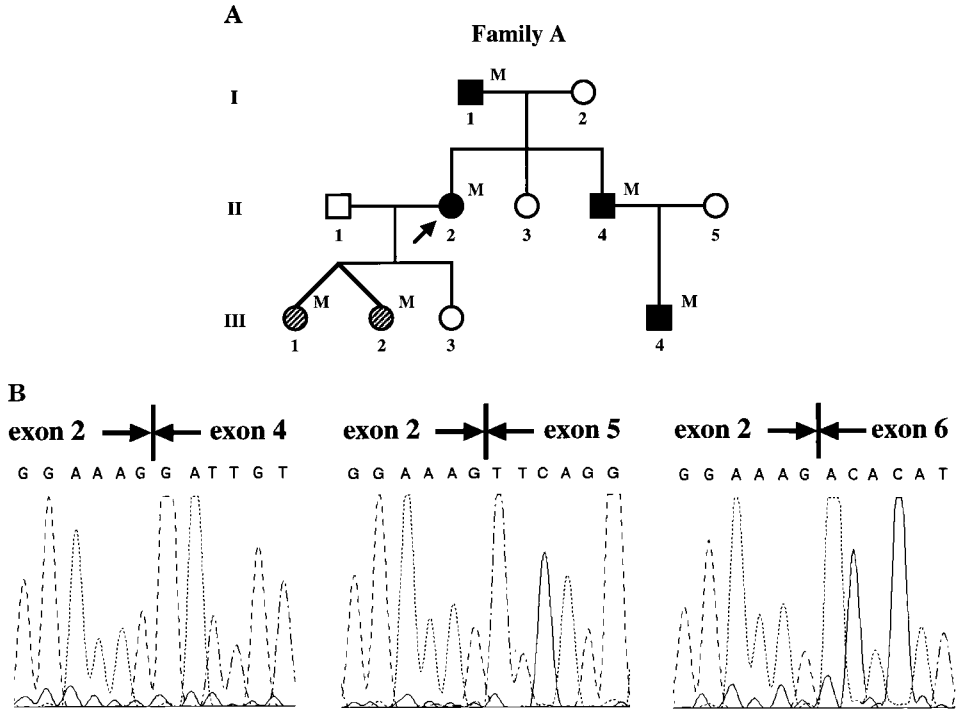

Fig 1. (A) Pedigree of Family A with cDNA sequencing data of the GTP cyclohydrolase I gene (GCH1). Squares = *males;* circles = *females;* solid symbols = *patients with dopa-responsive dystonia (DRD);* hatched symbols = *twins with probable foot dystonia only after extreme exercise (see Patients and Methods for details). The proband is indicated by an* arrow. *Mutant mRNA transcripts detected by sequencing of subcloned GCH1 cDNA are shown at the upper right of the symbols by* M. *(B) Sequence analysis of subcloned GCH1 cDNA in Family A. In each of 6 subjects (4 affected members [I-1, II-2, II-4, and III-4] and both twins [III-1 and III-2]), two mRNA transcripts (the normal cDNA and a mutant cDNA lacking exon 3 [left]) were detected. In addition, a mutant cDNA lacking exons 3 and 4 (middle) was identified in individual III-4 and a mutant cDNA lacking exons 3, 4, and 5 (right) was found in individual II-4.*

only one family had two point mutations on one allele; the functional significance of these mutations remains uncertain because mRNA was not analyzed.[9,12,13] The poly(A) signal on the 3′ end was also sequenced in six of the 10 pedigrees, but none of the six pedigrees demonstrated mutations.[12] These previous negative findings of GCH1 analyses would have made the possibility of a mutation in, as yet undefined, regulatory genes in coding region mutation-negative pedigrees with DRD more likely. However, our finding of the deletion in Family A suggests that the possibility of a large deletion in GCH1, which is undetectable by the conventional genomic DNA sequence analysis of this gene, should be considered before examination of a mutation in other genes.

In Family A, our data indicate that the large GCH1 deletion probably includes the entire region of the exon 3–PCR product (from intron 2 to intron 3); however, we cannot completely exclude the possibility that a small part of one of the ends of this region might not be deleted. Sequencing of the whole introns 2 and 3 was not conducted, because the normal intronic sequence of these relatively long introns is unknown. In addition to the large genomic deletion with probable involvement of both splicing junctions of exon 3, variable skipping of the downstream exon(s) (exon 4 or exons 4 and 5) occurred in some mutant mRNA transcripts in Family A. A mutation that abolishes a splice site typically causes loss of an adjacent single exon because of defective splicing.[5,7,8,18] However, skipping of the additional exon(s) and complex patterns of exon skipping have been reported in other genes.[18–20] Although we cannot explain the reason for skipping of exon 4 or exons 4 and 5, the large GCH1 deletion may have had an influence on the recognition or processing of the downstream exons.

All of the mutant alleles found in our four DRD families most likely produce dysfunctional GTPCH proteins. However, the reason for intrafamilial phenotypic variability in Family A (4 affected members vs relatively unaffected twins) is unknown as is the case in many previously reported DRD pedigrees that showed marked variation in expressivity of GCH1 mutations.[8,12,14] Other genetic and/or environmental factors probably modulate the outcome of a GCH1 mutation.

In conclusion, our finding of a large GCH1 deletion

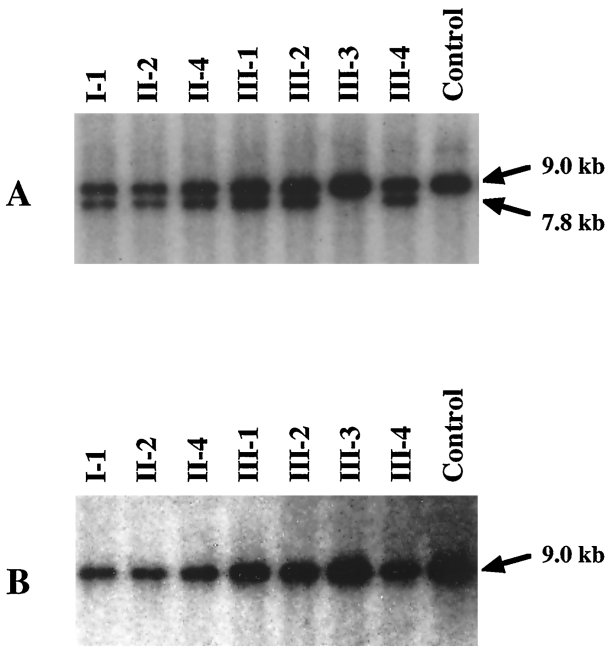

Fig 2. Southern blotting of Hind*III-digested genomic DNA in Family A. (A) By using the polymerase chain reaction (PCR) product for exon 2 of the GTP cyclohydrolase I gene (GCH1) as a probe, an aberrant band (7.8 kb) was detected in 6 subjects (4 affected members [I-1, II-2, II-4, and III-4] and both twins [III-1 and III-2]) but not in an unaffected sibling (III-3) and a normal control (for individual numbers, see Fig 1A). This abnormal band was not observed in another unaffected sibling (II-3), 2 spouses (I-2, II-5), and 19 other normal control subjects examined (data not shown). (B) By using the GCH1 exon 3–PCR product as a probe, the 7.8-kb aberrant fragment disappeared, whereas a normal fragment (9.0 kb) shown in A was also hybridized with this probe.*

in one of the four DRD families examined indicates that at least some dominantly inherited coding region mutation-negative patients with DRD will have a GCH1 defect caused by a large genomic deletion in this gene. We recommend conducting not only genomic DNA but also cDNA sequence analysis of GCH1 to establish the molecular genetic diagnosis of patients with this treatable disorder.

This study was supported in part by the Centre for Addiction and Mental Health Foundation.

We thank Linda DiStefano for technical assistance.

Presented in part in Works in Progress at the 124th Annual Meeting of the American Neurological Association, October 10–13, 1999, Seattle, WA.

References

1. Furukawa Y, Kish SJ. Dopa-responsive dystonia: recent advances and remaining issues to be addressed. Mov Disord 1999; 14:709–715
2. Ichinose H, Ohye T, Takahashi E, et al. Hereditary progressive dystonia with marked diurnal fluctuation caused by mutations in the GTP cyclohydrolase I gene. Nat Genet 1994;8:236–242
3. Bartholomé K, Lüdecke B. Mutations in the tyrosine hydroxylase gene cause various forms of L-dopa responsive dystonia. Adv Pharmacol 1998;42:48–49
4. Ichinose H, Ohye T, Segawa M, et al. GTP cyclohydrolase I gene in hereditary progressive dystonia with marked diurnal fluctuation. Neurosci Lett 1995;196:5–8
5. Furukawa Y, Shimadzu M, Rajput AH, et al. GTP-cyclohydrolase I gene mutations in hereditary progressive and dopa-responsive dystonia. Ann Neurol 1996;39:609–617
6. Hirano M, Imaiso Y, Ueno S. Differential splicing of the GTP cyclohydrolase I RNA in dopa-responsive dystonia. Biochem Biophys Res Commun 1997;234:316–319
7. Furukawa Y, Lang AE, Trugman JM, et al. Gender-related penetrance and de novo GTP-cyclohydrolase I gene mutations in dopa-responsive dystonia. Neurology 1998;50:1015–1020
8. Steinberger D, Weber Y, Korinthenberg R, et al. High penetrance and pronounced variation in expressivity of *GCH1* mutations in five families with dopa-responsive dystonia. Ann Neurol 1998;43:634–639
9. Tamaru Y, Hirano M, Ito H, et al. Clinical similarities of hereditary progressive/dopa responsive dystonia caused by different types of mutations in the GTP cyclohydrolase I gene. J Neurol Neurosurg Psychiatry 1998;64:469–473
10. Illarioshkin SN, Markova ED, Slominsky PA, et al. The GTP cyclohydrolase I gene in Russian families with dopa-responsive dystonia. Arch Neurol 1998;55:789–792
11. Jeon BS, Jeong J-M, Park S-S, et al. Dopamine transporter density measured by [^{123}I]β-CIT single-photon emission computed tomography is normal in dopa-responsive dystonia. Ann Neurol 1998;43:792-800
12. Bandmann O, Valente EM, Holmans P, et al. Dopa-responsive dystonia: a clinical and molecular genetic study. Ann Neurol 1998;44:649–656
13. Hirano M, Komure O, Ueno S. A novel missense mutant inactivates GTP cyclohydrolase I in dopa-responsive dystonia. Neurosci Lett 1999;260:181–184
14. Brique S, Destée A, Lambert J-C, et al. A new GTP-cyclohydrolase I mutation in an unusual dopa-responsive dystonia, familial form. Neuroreport 1999;10:487–491
15. Nomura T, Ohtsuki M, Matsui S, et al. Isolation of a full-length cDNA clone for human GTP cyclohydrolase I type 1 from pheochromocytoma. J Neural Transm Gen Sect 1995; 101:237–242
16. Maier J, Witter K, Gütlich M, et al. Homology cloning of GTP-cyclohydrolase I from various unrelated eukaryotes by reverse-transcription polymerase chain reaction using a general set of degenerate primers. Biochem Biophys Res Commun 1995;212:705–711
17. Nygaard TG, Wilhelmsen KC, Risch NJ, et al. Linkage mapping of dopa-responsive dystonia (DRD) to chromosome 14q. Nat Genet 1993;5:386–391
18. Nakai K, Sakamoto H. Construction of a novel database containing aberrant splicing mutations of mammalian genes. Gene 1994;141:171–177
19. Naylor JA, Green PM, Montandon AJ, et al. Detection of three novel mutations in two haemophilia A patients by rapid screening of whole essential region of factor VIII gene. Lancet 1991; 337:635–639
20. Haire RN, Ohta Y, Strong SJ, et al. Unusual patterns of exon skipping in Bruton tyrosine kinase are associated with mutations involving the intron 17 3′ splice site. Am J Hum Genet 1997;60:798–807

Synphilin-1 Is Present in Lewy Bodies in Parkinson's Disease

Koichi Wakabayashi, MD,*
Simone Engelender, MD, PhD,†¶
Makoto Yoshimoto, PhD,‡ Shoji Tsuji, MD,§
Christopher A. Ross, MD, PhD,†
and Hitoshi Takahashi, MD‖

α-Synuclein is believed to play an important role in Parkinson's disease (PD). Mutations in the α-synuclein gene are responsible for familial forms of PD and α-synuclein protein is a major component of Lewy bodies in patients with sporadic PD. Synphilin-1 is a novel protein that we have previously found to associate in vivo with α-synuclein. We now show that synphilin-1 is present in Lewy bodies of patients with PD. Our data suggest that synphilin-1 could play a role in Lewy body formation and the pathogenesis of PD.

Wakabayashi K, Engelender S, Yoshimoto M, Tsuji S, Ross CA, Takahashi H. Synphilin-1 is present in Lewy bodies in Parkinson's disease. Ann Neurol 2000;47:521–523

Parkinson's disease (PD), one of the most common neurodegenerative disorders, is usually sporadic, but, in familial forms, can be caused by mutations in the α-synuclein gene.[1–4] Two mutations, A53T and A30P, were found in different families with PD. The A53T mutation segregated with the disease phenotype in four mediterranean families,[1] and the A30P mutation was found in a family of German origin.[2]

Lewy bodies (LBs) are neuronal cytoplasmic inclusions that are highly characteristic of both sporadic and familial PD. α-Synuclein protein is a major component of LBs.[5–9] In addition to α-synuclein, several proteins have been detected in LBs from PD, including neurofilaments and ubiquitin.[10,11] However, the precise molecular composition of LBs and the mechanism of LB formation still remain to be clarified.

α-Synuclein is a presynaptic protein enriched in the brain.[12] Although a role in synaptic vesicle transport has been postulated,[13] the function of α-synuclein is still unknown. Recently, Engelender and colleagues[14] identified a novel protein, called synphilin-1, that associates with α-synuclein, and promotes the formation of eosinophilic cytoplasmic inclusions resembling LBs when cotransfected with α-synuclein in mammalian cells. Here, we report that synphilin-1 is a component of LBs in postmortem human patient brain tissue.

Materials and Methods

Preparation of Synphilin-1 Antibody

Rabbits were immunized with glutathione *S*-transferase (GST)-synphilin-1 (amino acids 30–543; GenBank AF 076929). Immune serum was filtered through a GST-Sepharose 4B column to eliminate anti-GST antibodies. To purify synphilin-1 antibodies, precleared serum was incubated overnight with anti–GST-synphilin-1 immobilized on polyvinylidene difluoride membrane strips. After extensive washings with 500 mM NaCl, synphilin-1 antibodies were eluted from the strips with 100 mM glycine, pH 2.5, and dialyzed against phosphate-buffered saline.

Western Blot Analysis

Postmortem frozen tissues from the substantia nigra of 2 PD patients and 2 controls were homogenized, and protein lysates (50 μg) were fractionated on 4% to 15% gradient sodium dodecyl sulfate–polyacrylamide gel electrophoresis and transferred to polyvinylidene difluoride membranes (Schleicher and Schuell) at 300 mA for 16 hours. The blots were processed as described previously[15]; 1 μg/ml purified polyclonal synphilin-1 antibody was used as primary antibody. Western blots were developed with enchanced chemiluminescence detection reagents and the yielded luminescence was captured on a hyperfilm (Amersham). The synphilin-1 signal is shown in black and white.

Immunohistochemistry

Five patients with neuropathologically confirmed PD (age range, 60–82 years), 3 patients with Alzheimer's disease (AD) (ages, 77, 81, and 86 years), and 5 control subjects (age range, 56–85 years) were used. Brains were fixed with 4% paraformaldehyde, and blocks were cut from various cortical and subcortical regions, embedded in paraffin, sectioned, and then stained with hematoxylin and eosin and by the Kluver-Barrera method. In each case, 4-μm-thick sections of the temporal lobe, midbrain, and upper pons were cut and immunostained by using the avidin-biotin-peroxidase complex method with diaminobenzidine as a chromogen. The antibodies used were polyclonal antibodies against synphilin-1 (diluted 1:1,000) and α-synuclein (NACP-5[16]; diluted 1:1,000). Synphilin-1 and α-synuclein immunolabeling signals are shown in brown.

Results

Western blot analysis showed that the anti-synphilin-1 antibody recognized a band of 90 kd in our tissues (Fig

From the *Brain Disease Research Center, and Departments of §Neurology and ‖Pathology, Brain Research Institute, Niigata University, Niigata, and ‡Molecular Biology Laboratory, Taisho Pharmaceutical Co Ltd, Ohmiya, Japan; and †Division of Neurobiology, Department of Psychiatry, Johns Hopkins University School of Medicine, Baltimore, MD.

Received Sep 20, 1999, and in revised form Nov 18. Accepted for publication Nov 19, 1999.

¶Present address: Departamento de Anatomia, Universidade Federal do Rio de Janeiro, Ilha do Fundao, Brazil.

Address correspondence to Dr Takahashi, Department of Pathology, Brain Research Institute, Niigata University, 1-757 Asahimachi, Niigata 951-8585, Japan.

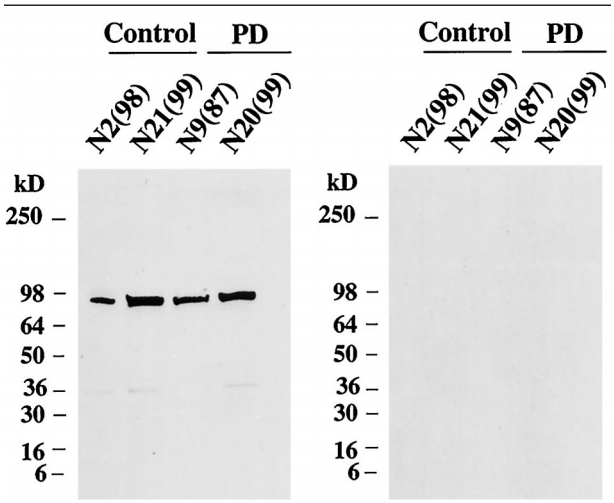

Fig 1. Western blot analysis of anti-synphilin-1 in postmortem human brain tissue. Immunoblot of protein lysate from human midbrain samples (control and Parkinson's disease [PD]) detected with 1 μg/ml synphilin-1 antibody (left) and 1 μg/ml synphilin-1 antibody preabsorbed with 10 μg/ml GST-synphilin-1 fusion protein (right). GST = glutathione S-transferase.

1, left), in accordance with the predicted molecular mass of human synphilin-1.[14] This band is specific because it disappeared when the antibody was preincubated with antigen (see Fig 1, right).

We studied formalin-fixed, paraffin-embedded sections of the brain issues from 5 patients with PD, 3 with AD, and 5 normal control subjects (all clinically and pathologically confirmed cases). We stained the sections with polyclonal antibodies against synphilin-1[14] and α-synuclein (NACP-5).[16] NACP-5 was raised against a synthetic peptide that corresponded to residues 114–131 of human α-synuclein and specifically recognized α-synuclein (data not shown), with results similar to other published antibodies.[5,6]

Synphilin-1 colocalizes with α-synuclein within rat cortical neurons, and synphilin-1 immunostaining showed a neuropil distribution in a punctate pattern throughout the brain of the control subjects that closely resembles the pattern for α-synuclein in controls (Engelender and colleagues[14]; Engelender S, et al, unpublished data). In PD, most LBs observed inside and outside the substantia nigra (Fig 2A and B) were positive for synphilin-1. Serial sections stained with anti-synphilin-1 and hematoxylin and eosin revealed that approximately 80% to 90% of LBs were positive for synphilin-1. These LBs often showed intense staining in their central cores, with their peripheral portions unstained. Immunolabeling was specific, because it was abolished on sections in which the primary antibody was preabsorbed with GST-synphilin-1 fusion protein (see Fig 2C) or the primary antibody was replaced by preimmune serum (data not shown). Anti-α-synuclein antibodies showed homogeneous label or intense staining in peripheral portions of LBs (see Fig 2D). Lewy neurites, which were positive for α-synuclein, were synphilin-1

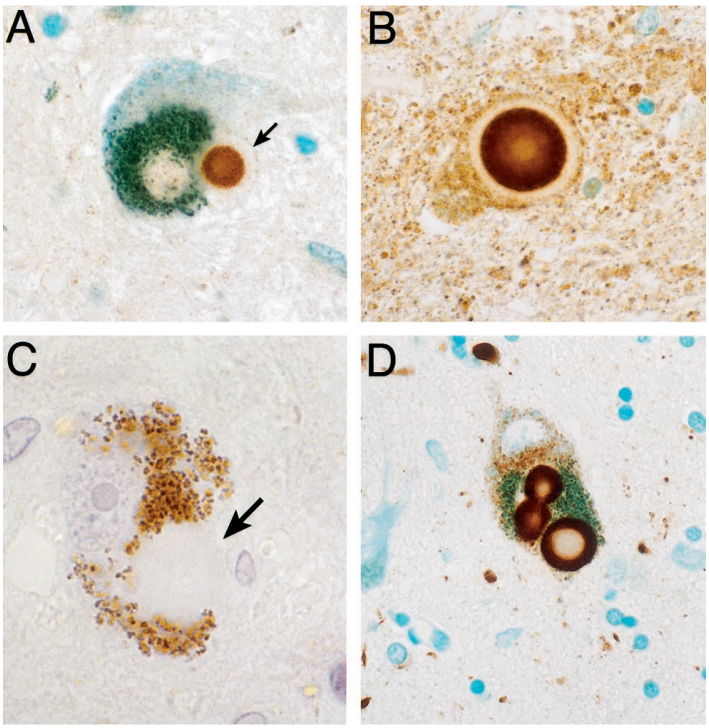

Fig 2. Synphilin-1 and α-synuclein immunoreactivity in the brain from patients with Parkinson's disease. (A) A substantia nigra pigmented neuron with a synphilin-1–positive Lewy body (arrow). *(B) A synphilin-1–positive Lewy body in the oculomotor nucleus. (C) A pigmented neuron from substantia nigra with a Lewy body* (arrow) *that showed no immunolabeling when reacted with synphilin-1 antibody preabsorbed with antigen GST-synphilin-1 fusion protein. (D) Locus ceruleus pigmented neurons that contain α-synuclein–positive Lewy bodies. Magnification: ×330 (A and B), ×495 (C), and ×240 (D); all before 25% reduction. All sections counterstained with methyl green (pigment granules are green) except C, which was counterstained with cresyl violet. GST = glutathione S-transferase.*

negative. No synphilin-1 immunoreactivity was found in the senile plaques or neurofibrillary tangles in AD.

Discussion

LBs are neuronal cytoplasmic inclusions that consist of filaments and granular structures, which contain α-synuclein as well as other proteins.[10] In this study, we have identified synphilin-1 as a component of LBs in patients with PD. That synphilin-1 was not found in AD protein aggregates indicates specificity and suggests that synphilin-1 deposition could be specific for lesions in which α-synuclein is a major component. Although synphilin-1 was detected in most LBs analyzed, we did not observe deposition of synphilin-1 in Lewy neurites. Lewy neurites are dystrophic neurites that occur in addition to LBs. The role of Lewy neurites is still unknown, but they have a similar immunohistochemical profile as LBs.[5] Thus, our data suggest that LBs and Lewy neurites may have a heterogeneous composition and that they could be associated with different aspects of the disease.

In our material, the central cores of LBs often contained synphilin-1, which suggests that synphilin-1 is not secondarily deposited on preexisting inclusions and that it could play a role in LB formation. Synphilin-1 was detected in 80% to 90% of LBs not only in substantia nigra but also in other regions of the brain characteristically affected in PD, such as locus ceruleus, oculomotor nucleus, and cerebral cortex. That synphilin-1 could not be detected in 10% to 20% of LBs could be the result of low sensitivity of the synphilin-1 antibody used for this study. An alternative explanation is that LB formation does not require synphilin-1. Generation of other synphilin-1 antibodies may help clarify the exact extent of synphilin-1 deposition in LBs.

In cell culture, synphilin-1 promotes the formation of inclusions, which can be labeled for both α-synuclein and synphilin-1. Our data suggest that an analogous process may occur in vivo. α-Synuclein can aggregate by itself in vitro,[17–19] but relatively high concentrations are required, which suggests that synphilin-1 could accelerate the deposition of α-synuclein within the cell.

The genetic loci for most PD cases have not been identified yet.[20] Our data provide a rationale to a search for mutations in synphilin-1 as possible contributors to familial PD. Similarly to α-synuclein, the function of synphilin-1 is unknown. The presence of ankyrin domains within synphilin-1 protein suggests that it could be a cytoskeletal-related protein. Future studies on the function of synphilin-1 may be helpful to understand the normal function of α-synuclein as well as to clarify the role of α-synuclein and synphilin-1 in the formation of LBs and the pathogenesis of PD.

This work was supported by NIH grants NS 38377 and NS 16375, and a research grant from the Research Committee for CNS Degenerative Diseases from the Ministry of Health and Welfare, Japan, and Grants-in-Aid Scientific Research from the Ministry of Education, Science, Sports and Culture, Japan.

References

1. Polymeropoulos MH, Lavedan C, Leroy E, et al. Mutation in the α-synuclein gene identified in families with Parkinson's disease. Science 1997;276:2045–2047
2. Krüger R, Kuhn W, Muller T, et al. Ala30Pro mutation in the gene encoding α-synuclein in Parkinson's disease. Nat Genet 1998;8:106–108
3. Dunnett SB, Björklund A. Prospects for new restorative and neuroprotective treatments in Parkinson's disease. Nature 1999; 399:A32–A39
4. Hardy J, Gwinn-Hardy K. Genetic classification of primary neurodegenerative disease. Science 1998;282:1075–1079
5. Spillantini MG, Schmidt ML, Lee VM, et al. α-Synuclein in Lewy bodies. Nature 1997;388:839–840
6. Takeda A, Mallory M, Sundsmo M, et al. Abnormal accumulation of NACP/alpha-synuclein in neurodegenerative disorders. Am J Pathol 1998;152:367–372
7. Baba M, Nakajo S, Tu PH, et al. Aggregation of α-synuclein in Lewy bodies of sporadic Parkinson's disease and dementia with Lewy bodies. Am J Pathol 1998;152:879–884
8. Wakabayashi K, Hayashi S, Kakita A, et al. Accumulation of α-synuclein/NACP is a cytopathological feature common to Lewy body disease and multiple system atrophy. Acta Neuropathol 1998;96:445–452
9. Jellinger K. Overview of morphological changes in Parkinson's disease. Adv Neurol 1986;45:1–18
10. Pollanen MS, Dickson DW, Bergeron C. Pathology and biology of the Lewy body. J Neuropathol Exp Neurol 1993;52:183–191
11. Goldman JE, Yen SH, Chiu FC, Peress NS. Lewy bodies of Parkinson's disease contain neurofilament antigens. Science 1983;221:1082–1084
12. Maroteaux L, Scheller RH. The rat brain synucleins: family of proteins transiently associated with neuronal membrane. Mol Brain Res 1991;11:335–343
13. Jensen PH, Nielsen MS, Jakes R, et al. Binding of alpha-synuclein to brain vesicles is abolished by familial Parkinson's disease mutation. J Biol Chem 1998;273:26292–26294
14. Engelender S, Kaminsky Z, Guo X, et al. Synphilin-1 associates with α-synuclein and promotes the formation of cytosolic inclusions. Nat Genet 1999;22:110–114
15. Engelender S, Sharp AH, Colomer V, et al. Huntingtin-associated protein 1 (HAP1) interacts with dynactin p150^{Glued} and other cytoskeletal related proteins. Hum Mol Genet 1997; 13:2205–2212
16. Wakabayashi K, Hayashi S, Yoshimoto M, et al. NACP/α-synuclein-positive filamentous inclusions in astrocytes and oligodendrocytes of Parkinson's disease brains. Acta Neuropathol 2000;99:14–20
17. Conway KA, Harper JD, Lansbury PT. Accelerated in vitro fibril formation by a mutant alpha-synuclein linked to early-onset Parkinson disease. Nat Med 1998;4A:1318–1320
18. El-Agnaf OM, Jakes R, Curran MD, Wallace A. Effects of the mutations Ala30 to Pro and Ala53 to Thr on the physical and morphological properties of alpha-synuclein protein implicated in Parkinson's disease. FEBS Lett 1998;440:67–70
19. Narhi L, Wood SJ, Steavenson S, et al. Both familial Parkinson's disease mutations accelerate α-synuclein aggregation. J Biol Chem 1999;274:9843–9846
20. Farrer M, Gwinn-Hardy K, Hutton M, Hardy J. The genetics of disorders with synuclein pathology and parkinsonism. Hum Mol Genet 1999;8:1901–1905

Nitration of Manganese Superoxide Dismutase in Cerebrospinal Fluids Is a Marker for Peroxynitrite-Mediated Oxidative Stress in Neurodegenerative Diseases

Koji Aoyama, MD,*† Kazuo Matsubara, PhD,† Yasunori Fujikawa, MD,* Yukio Nagahiro, MD, PhD,‡ Keiko Shimizu, MD, PhD,§ Nobuyuki Umegae, MD,* Nobumasa Hayase, PhD,† Hiroshi Shiono, MD, PhD,§ and Shotai Kobayashi, MD, PhD*

Peroxynitrite can nitrate tyrosine residues of proteins. We examined nitrotyrosine-containing proteins in cerebrospinal fluid of 66 patients with neurogenic disease by immunoblot analysis. Nitrated tyrosine residue–containing protein was observed in the cerebrospinal fluid and was concluded to be manganese superoxide dismutase (Mn-SOD). The nitrated Mn-SOD level was strikingly elevated in amyotrophic lateral sclerosis patients and was slightly increased in Alzheimer's and Parkinson's disease patients, whereas an elevated Mn-SOD level was observed only in progressive supranuclear palsy group.

Aoyama K, Matsubara K, Fujikawa Y, Nagahiro Y, Shimizu K, Umegae N, Hayase N, Shiono H, Kobayashi S. Nitration of manganese superoxide dismutase in cerebrospinal fluids is a marker for peroxynitrite-mediated oxidative stress in neurodegenerative diseases. Ann Neurol 2000;47:524–527

Oxidative stress has been suggested to be involved in the pathogenesis of various neurodegenerative diseases. Supporting evidence of oxidative stress comes from a variety of in vitro studies that show that free radicals are capable of mediating neuronal degeneration. Nitric oxide (NO) is cytotoxic, especially to neurons, under certain conditions. NO contains an unpaired electron that can combine with free radicals such as superoxide to form peroxynitrite. Peroxynitrite leads to lipid peroxidation, dysfunction of enzyme, and DNA damage.[1,2] Particularly in mitochondria, peroxynitrite-mediated injury induces inhibition of the electron transport chain,[3] followed by opening of the permeability transition pore located on the mitochondrial inner membrane. These events cause cell death.[4]

Recent reports have demonstrated the widespread nitration of tyrosine residues in Alzheimer's disease (AD) and Parkinson's disease (PD) brains.[5,6] When transition metal ions or certain metalloproteins such as superoxide dismutase (SOD) are present, the rate of tyrosine nitration is high.[7] This nitration has been suggested to be pathologically important in certain neurodegenerative diseases. Although peroxynitrite can react with both copper/zinc-SOD (Cu/Zn-SOD) and Mn-SOD, the latter is inactivated by the nitration.[7] The activities of Mn-SOD and Cu/Zn-SOD in cerebrospinal fluid (CSF) are correlated with certain neurogenic diseases.[8,9] These findings expanded our interests toward the study of tyrosine nitration in the protein of CSF. Hence, we analyzed nitrotyrosine-containing proteins by using nitrotyrosine antibody in the CSF of patients who demonstrated intracerebral degenerative processes.

Patients and Methods

Patients

This study included 66 neurogenic patients with PD, AD, amyotrophic lateral sclerosis (ALS), progressive supranuclear palsy (PSP), spinocerebellar degeneration, cerebrovascular disease, and normal pressure hydrocephalus (Table). All patients were admitted to our hospitals and the diagnoses were based on neurological history, neurological examination, and laboratory test, including computed tomography and magnetic resonance imaging, in accordance with the diagnostic criteria.[10–14] Spinocerebellar degeneration included olivopontocerebellar atrophy, late cerebellar cortical atrophy, Shy-Drager syndrome, and dentatorubro-pallidoluysian atrophy. The CSF samples from patients with cerebrovascular disease, which included those with cerebral infarction or cerebral hemorrhage, were withdrawn more than half a month after their onsets. The control group consisted of 6 patients without any neurodegenerative or cerebrovascular disease. We carefully excluded patients who were diagnosed ambiguously or those suffering from inflammatory diseases. Because there were no available nitrotyrosine-containing proteins as standards, the CSF sample of a 37-year-old man who was healthy and had not taken any drugs was used as an internal standard in each analysis.

Western Blot Analysis

CSF (100 μl) was added to 200 μl of buffer, which consisted of 75 mM Tris-HCl (pH 6.8), 15% glycerol, 1.5% sodium dodecyl sulfate (SDS), 0.16 M sucrose, 0.5 mM EGTA, 2.5 mM NaN_3, 0.1 mM phenylmethanesulfonyl fluoride, 10 μM leupeptin, 750 nM pepstain A, 1.5% β-mercaptoethanol, and 0.00375% bromophenol blue. The mixture was then heated for 90 seconds at 95°C. Proteins

From the *Department of Internal Medicine III, Shimane Medical University, Izumo; Departments of †Hospital Pharmacy and Pharmacology and §Legal Medicine, Asahikawa Medical College, Asahikawa; and ‡Department of Orthopedics, Yamaguchi University, Ube, Japan.

Received May 3, 1999, and in revised form Nov 22. Accepted for publication Nov 22, 1999.

Address correspondence to Dr Matsubara, Department of Hospital Pharmacy and Pharmacology, Asahikawa Medical College, Asahikawa 078-8510, Japan.

Table. Patient Characteristics and the Relative Levels of 96-kd Proteins Stained by Nitrotyrosine and Mn-SOD Antibodies

	n	Male/Female	Age (yr)	CSF protein (mg/dl)	Nitrotyrosine Positive	Mn-SOD
Control	6	3/3	63.7 ± 8.10	35.7 ± 8.59	1.26 ± 0.17	1.94 ± 0.42
PD	10	2/8	73.4 ± 2.95	47.5 ± 5.25	2.26 ± 0.26[a]	2.45 ± 0.36
AD	6	4/2	65.5 ± 8.78	61.4 ± 13.6	2.35 ± 0.21[b]	2.59 ± 0.60
ALS	8	7/1	62.4 ± 6.12	54.3 ± 11.3	3.55 ± 0.64[b]	1.94 ± 0.46
PSP	6	4/2	69.3 ± 3.77	46.1 ± 8.11	1.77 ± 0.37	4.43 ± 0.68[a]
SCD	10	3/7	60.7 ± 3.41	32.0 ± 4.0	1.58 ± 0.24	1.65 ± 0.17
CVD	22	18/4	70.4 ± 1.83	39.1 ± 3.45	1.66 ± 0.16	2.26 ± 0.26
NPH	4	4/0	73.5 ± 2.85	26.5 ± 2.13	2.42 ± 0.71	2.10 ± 0.70

Data are mean ± SEM values. The levels of nitrotyrosine- and SOD-positive proteins were presented as relative ratios to those in the internal standard patient.

[a]$p < 0.02$ and [b]$p < 0.01$, compared with the control group, by the Mann-Whitney *U* test.

Mn-SOD = manganese superoxide dismutase; CSF = cerebrospinal fluid; PD = Parkinson's disease; AD = Alzheimer disease; ALS = amyotrophic lateral sclerosis; PSP = progressive supranuclear palsy; SCD = spinocerebellar degeneration; CVD = cerebrovascular disease; NPH = normal pressure hydrocephalus.

were separated by 10% SDS-polyacrylamide gel electrophoresis (SDS-PAGE) and electrophoretically transferred to a nitrocellulose membrane. The membrane was sequentially treated with Block Ace (Dainihonseiyaku, Osaka, Japan) and horseradish peroxidase–conjugated anti-rabbit Ig from donkey (1:10,000 dilution; Amersham) in 10 mM Tris/saline/0.05% Tween 20, pH 7.4 (TBS-T), that contained 1% bovine serum albumin. After washing six times with TBS-T, the membrane was incubated overnight at 4°C with rabbit polyclonal nitrotyrosine antibody (2 μg/ml; Upstate Biotechnology, New York, NY) in 1% bovine serum albumin/TBS-T/0.02% NaN_3. The membrane was washed again six times and was probed with horseradish peroxidase–linked anti-rabbit Ig antibody. The membrane was washed 12 times and then treated with chemiluminescent reagents (Amersham, Little Chalfont, UK), followed by immediate exposure to x-ray film. The protein-transferred membrane was also treated with sheep polyclonal anti-human Mn-SOD (1:1,000 dilution; Calbiochem, San Diego, CA) antibody. Further treatment of the membrane was the same as above, using horseradish peroxidase–linked anti-sheep Ig antibody from rabbit (Amersham). The x-ray film was scanned by using a densitograph system. The levels of nitrotyrosine- and SOD-positive proteins were presented as relative density ratios to those of the internal standard. The protein concentration was measured by the Bradford assay.[15] Continuous variables were compared by the Mann-Whitney *U* test and Spearman's rank correlation coefficient.

Nitrotyrosine Immunoprecipitation

CSF (1 ml) was precleared with 50 μl protein A–agarose (Oncogene, Cambridge, UK). The supernatant was incubated overnight with nitrotyrosine antibody at 4°C. The immune complexes were precipitated with 75 μl of protein A–agarose for 90 minutes at 4°C. The pellet was washed three times with buffer consisting of phosphate-buffered saline (pH 7.4). After centrifugation, the pellet was resuspended in sample buffer. The sample was heated at 95°C for 90 seconds or boiled for 2 minutes to dissociate immune complexes. The supernatant was analyzed with 15% SDS-PAGE, followed by immunodetection by using nitrotyrosine, Mn-SOD, and Cu/Zn-SOD (Calbiochem; Wako, Osaka, Japan) antibodies.

Results

The mean age and CSF protein in each group were not significantly different (see Table). After immunoprecipitation, the nitrotyrosine antibody recognized 96-kd and 40-kd proteins (Fig 1A). The Mn-SOD antibody also stained 96- and 40-kd proteins (see Fig 1B). Strong heat treatment before SDS-PAGE dissociated the 96-kd protein into 48- and 24-kd bands immunostained by both nitrotyrosine and Mn-SOD antibodies. The proteins that have 30- and 36-kd molecular mass also appeared after the strong heat treatment of the sample. The Cu/Zn-SOD antibody did not recognize any protein after immunoprecipitation with nitrotyrosine antibody (data not shown).

Figure 2 shows quantitative immunodetections with nitrotyrosine and Mn-SOD antibodies after 10% SDS-PAGE. The 96-kd band was clearly detected by both antibodies. The other bands, shown in 15% SDS-PAGE after immunoprecipitation (see Fig 1), were not observed. The 96-kd band was not detected by using nitrotyrosine antibody preincubated with 3-nitrotyrosine. Quantitative analysis was performed on the 96-kd protein, and relative levels are summarized in the Table. Statistical analysis revealed that the level of the 96-kd protein detected by nitrotyrosine antibody was higher in PD ($p < 0.02$), AD ($p < 0.01$), and ALS ($p < 0.01$) groups than in the controls. The level of the nitrated 96-kd protein in patients with PSP, spinocerebellar degeneration, cerebrovascular disease, and normal pressure hydrocephalus was almost equal to that in control group. In Mn-SOD analysis, PSP patients showed significantly higher levels than the control group ($p < 0.01$). Neither sex difference nor age-related correlation in the 96-kd protein, detected by either nitrotyrosine antibody or Mn-SOD antibody,

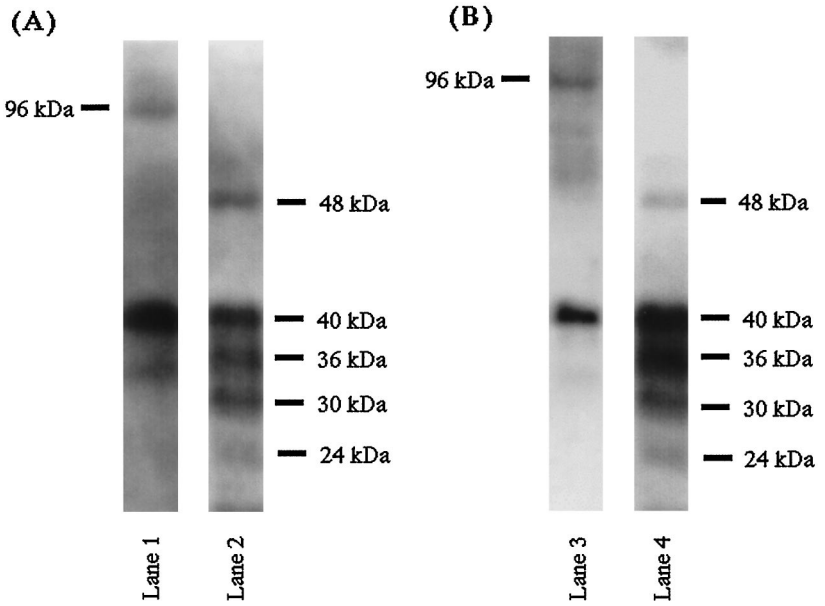

Fig 1. Sodium dodecyl sulfate–polyacrylamide gel electrophoresis (15% polyacrylamide gel) with western blot analysis, using nitrotyrosine (A) or manganese superoxide dismutase (B) antibodies after immunoprecipitation by nitrotyrosine antibody. The samples in lanes 1 and 3 were heated at 95°C for 90 seconds. The samples in lane 2 and 4 were boiled for 2 minutes. After the strong heat treatment, the 96-kd band in lanes 1 and 3 disappeared and appeared as 24- and 48-kd bands, which were considered as monomeric and dimeric manganese superoxide dismutase, respectively.

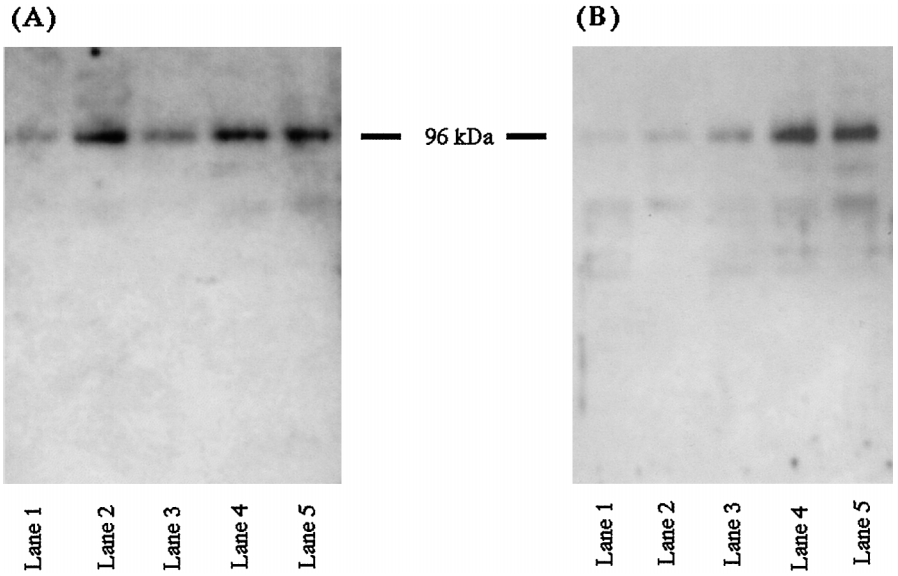

Fig 2. A typical sodium dodecyl sulfate–polyacrylamide gel electrophoresis (10% polyacrylamide gel) with western blot analysis, using nitrotyrosine (A) and manganese superoxide dismutase (B) antibodies. (A) Lane 1 = normal control; lane 2 = amyotrophic lateral sclerosis (ALS); lane 3 = cerebrovascular disease (CVD); lane 4 = Alzheimer's disease (AD); lane 5 = Parkinson's disease. (B) Lane 1 = normal control; lane 2 = ALS; lane 3 = CVD; lane 4 = progressive supranuclear palsy; lane 5 = AD.

was observed. The amount of nitrotyrosine-positive protein did not correlate with that of Mn-SOD.

Discussion

This is the first report that identifies a nitrotyrosine-containing protein in human CSF. The 96-kd protein recognized by the nitrotyrosine antibody was also stained by the Mn-SOD antibody. This 96-kd protein was dissociated into 48- and 24-kd proteins. Human Mn-SOD is a homotetramer (96 kd) containing one manganese atom and nine tyrosine residues in each subunit.[16] Thus, the 96-kd protein was considered to be a tetrameric Mn-SOD. The presence of Mn-SOD in CSF is supported by several reports.[8,9] However, sequencing of this protein by the microsequence technique failed because of insufficient sample amounts (data not shown). The proteins, which showed higher molecular mass bands than monomeric Mn-SOD (see Fig 1), stained only after immunoprecipitation. As the same phenomenon has been reported previously,[1] the characteristics of these bands were unknown. Peroxynitrite can also react with Cu/Zn-SOD. However, nitrated Cu/Zn-SOD, which should be 32 kd of homodimer proteins, was not observed.

Mn-SOD is a primary antioxidant enzyme that functions to remove superoxide radicals in mitochondria. Nitration of the tyrosine residue of Mn-SOD leads to inactivation of this enzyme[7] and an increase in

mitochondrial reactive oxygen species level, and consequently damage to other mitochondrial proteins and mtDNA.[17] In the present experiment, the amount of nitrated 96-kd protein, possibly Mn-SOD, was higher in PD, AD, and ALS groups than in the control group. These findings agree with recent reports that have demonstrated the widespread nitration of tyrosine residues in AD and PD brains. In PD patients, the presence of nitrotyrosine immunoreactivity has been observed in Lewy bodies within melanized neurons and in amorphous deposits associated with intact and degenerating neurons.[5] Good and associates[6] also reported colocalization of nitrotyrosine with the neurofibrillary tangles of AD. Amyloid β-peptide is known to stimulate NO production.[18] The signature of peroxynitrite involvement has also been demonstrated in ALS.[19] The cause of ALS has recently been linked to glutamate through convincing clinical evidence.[20] Motor neurons in the spinal cord are selectively injured by chronic exposure to glutamate and this is mediated by the formation of NO in nonmotor neurons.[21] Peroxynitrite may affect neurofilament assembly and cause neurofilament accumulation in motorneurons. The inactivation of Mn-SOD might be implicated in the pathogenesis of ALS. These observations could link oxidative stress caused by NO with a key pathological mechanism in PD, AD, and, especially, ALS. Nitration of Mn-SOD in CSF may be a marker for peroxynitrite-mediated oxidative stress in several neurodegenerative diseases. In contrast to PD, AD, and ALS, nitrated tyrosine residue–containing protein was not elevated in PSP patients, whereas obvious elevation of Mn-SOD was observed. This finding indicates that oxidative stress caused by factors other than NO might be one of the important factors in the pathogenesis of PSP, although the cause of this disease is quite obscure.

References

1. MacMillan-Crow LA, Crow JP, Kerby JD, et al. Nitration and inactivation of manganese superoxide dismutase in chronic rejection of human renal allografts. Proc Natl Acad Sci USA 1996;93:11853–11858
2. Szabo C, Zingarelli B, O'Connor M, Salzman AL. DNA strand breakage, activation of poly (ADP-ribose) synthetase, and cellular energy depletion are involved in the cytotoxicity of macrophages and smooth muscle cells exposed to peroxynitrite. Proc Natl Acad Sci USA 1996;93:1753–1758
3. Radi R, Rodriguez M, Castro L, Telleri R. Inhibition of mitochondrial electron transport by peroxynitrite. Arch Biochem Biophys 1994;308:89–95
4. Zoratti M, Szabo I. The mitochondrial permeability transition. Biochim Biophys Acta 1995;1241:139–176
5. Good PF, Hsu A, Werner P, et al. Protein nitration in Parkinson's disease. J Neuropathol Exp Neurol 1998;57:338–342
6. Good PF, Werner P, Hsu A, et al. Evidence of neuronal oxidative damage in Alzheimer's disease. Am J Pathol 1996;149: 21–28
7. Ischiropoulos H, Zhu L, Chen J, et al. Peroxynitrite-mediated tyrosine nitration catalyzed by superoxide dismutase. Arch Biochem Biophys 1992;298:431–437
8. Yoshida E, Mokuno K, Aoki S, et al. Cerebrospinal fluid levels of superoxide dismutases in neurological diseases detected by sensitive enzyme immunoassays. J Neurol Sci 1994;124:25–31
9. Strand T, Marklund SL. Release of superoxide dismutase into cerebrospinal fluid as a marker of brain lesion in acute cerebral infarction. Stroke 1992;23:515–518
10. Calne DB, Snow BJ, Lee C. Criteria for diagnosing Parkinson's disease. Ann Neurol 1992;32:S125–S127
11. American Psychiatric Association. Diagnostic and statistical manual of mental disorders. 4th ed. Washington, DC: American Psychiatric Association, 1994:133–155
12. Brooks BR. El Escorial World Federation of Neurology criteria for the diagnosis of amyotrophic lateral sclerosis. Subcommittee on Motor Neuron Diseases/Amyotrophic Lateral Sclerosis of the World Federation of Neurology Research Group on Neuromuscular Diseases and the El Escorial "Clinical Limits of Amyotrophic Lateral Sclerosis" Workshop contributors. J Neurol Sci 1994;124:S96–S107
13. Litvan I, Agid Y, Calne D, et al. Clinical research criteria for the diagnosis of progressive supranuclear palsy (Steele-Richardson-Olszewski syndrome): report of the NINDS-SPSP International Workshop. Neurology 1996;47:1–9
14. Hirayama K, Takayanagi T, Nakamura R, et al. Spinocerebellar degenerations in Japan: a nationwide epidemiological and clinical study. Acta Neurol Scand 1994;153:S1–S22
15. Bradford MM. A rapid and sensitive method for the quantitation of microgram quantities of protein utilizing the principle of protein-dye binding. Anal Biochem 1976;72:248–254
16. Borgstahl GE, Parge HE, Hickey MJ, et al. The structure of human mitochondrial manganese superoxide dismutase reveals a novel tetrameric interface of two 4-helix bundles. Cell 1992; 71:107–118
17. Kowaltowski AJ, Vercesi AE. Mitochondrial damage induced by conditions of oxidative stress. Free Radic Biol Med 1999;26: 463–471
18. Yang SN, Hsieh WY, Liu DD, et al. The involvement of nitric oxide in synergistic neuronal damage induced by beta-amyloid peptide and glutamate in primary rat cortical neurons. Chin J Physiol 1998;41:175–179
19. Beal MF, Ferrante RJ, Browne SE, et al. Increased 3-nitrotyrosine in both sporadic and familial amyotrophic lateral sclerosis. Ann Neurol 1997;42:644–654
20. Lin CL, Bristol LA, Jin L, et al. Aberrant RNA processing in a neurodegenerative disease: the cause for absent EAAT2, a glutamate transporter, in amyotrophic lateral sclerosis. Neuron 1998;20:589–602
21. Urushitani M, Shimohama S, Kihara T, et al. Mechanism of selective motor neuronal death after exposure of spinal cord to glutamate: involvement of glutamate-induced nitric oxide in motor neuron toxicity and nonmotor neuron protection. Ann Neurol 1998;44:796–807

A Single Nucleotide Polymorphism of Dopamine Transporter Gene Is Associated with Parkinson's Disease

Hiroyuki Morino, MD,* Toshitaka Kawarai, MD, PhD,*
Yuishin Izumi, MD,* Toshinari Kazuta, MD,†
Masaya Oda, MD,* Osamu Komure, MD, PhD,‡
Fukashi Udaka, MD, PhD,§
Masakuni Kameyama, MD, PhD,§
Shigenobu Nakamura, MD, PhD,*
and Hideshi Kawakami, MD, PhD*

We identified two polymorphisms out of all coding regions of the dopamine transporter gene. One existed in exon 9 (1215A/G) and another in exon 15 (1898T/C). The 1215G was significantly less frequent among patients with Parkinson's disease than the controls. Although the polymorphism caused no amino acid substitution, we concluded that it was associated with decreasing the susceptibility to Parkinson's disease through mechanisms other than the protein function of dopamine transporter.

Morino H, Kawarai T, Izumi Y, Kazuta T, Oda M, Komure O, Udaka F, Kameyama M, Nakamura S, Kawakami H. A single nucleotide polymorphism of dopamine transporter gene is associated with Parkinson's disease. Ann Neurol 2000;47:528–531

The precise pathogenesis of Parkinson's disease (PD) is still unknown, although genetic and toxic factors are postulated to contribute to the development of PD. Many previous studies have investigated genetic factors of PD. In recent twin studies, one large study indicated that no genetic component was evident when the disease began after age 50 years. However, genetic factors seemed to be important when disease began at or before age 50 years.[1] Another twin study that used positron emission tomography has revealed a strong genetic influence in PD.[2] Polymorphism of the α-synuclein gene,[3] the cytochrome P-450 CYP2D6 gene,[4] and glutathione transferase gene[5] have been investigated for causing sporadic PD. As models of toxic factors, 6-hydroxydopamine, and 1-methyl-4-phenylpyridinium (MPP^+), an active metabolite of 1-methyl-4-phenyl-1,2,3,6-tetrahydropyridine, cause parkinsonism.[6,7] These neurotoxins are taken into dopaminergic neurons via dopamine transporter (DAT).

The distribution of DAT resembles closely the pathological lesion of PD,[8,9] and the loss of dopaminergic neurons remarkably parallels the level of DAT mRNA.[10] Furthermore, mutants of DAT have been reported to enhance the transport of MPP^+ selectively.[11] These results show that DAT could be related to the vulnerability of dopaminergic neurons.

In our previous study, we determined structure and organization of the DAT gene.[12] To clarify whether polymorphisms of the DAT gene are associated with PD, we screened polymorphisms out of all coding regions of this gene by using the direct sequence and capillary electrophoresis system–based single-strand conformation polymorphism (CE-SSCP), and we compared their distribution between patients with PD and normal control subjects.

Subjects and Methods

Sample

We recruited 172 patients with sporadic PD (age at onset, 62.7 ± 8.1 years [mean ± SD]; female, 61.1%) who had clinically definite PD according to the criteria of Calne and colleagues.[13] The absence of familial cases of PD and early age at onset in this group was carefully assessed. We also examined 132 normal controls (age at the time of the examination, 63.7 ± 7.3 years; female, 50.0%). All subjects were Japanese, and there was no significant difference in the mean age and sex ratio between the two groups. Each subject was fully informed about and gave consent to this study.

Polymerase Chain Reaction

Genomic DNA was prepared from leukocytes by standard methods.[14] Expand High Fidelity PCR System (Boehringer Mannheim, Mannheim, Germany) was used for polymerase chain reaction (PCR), and PCR was performed according to the manufacturer's manual. An aliquot of genomic DNA (60 ng) was used for each 20 μl of PCR solution. Primers for PCR will be demonstrated elsewhere.

Direct Sequence and CE-SSCP

Direct sequence analysis was performed by using Sequencing Pro (Toyobo, Osaka, Japan). CE-SSCP analysis was performed as described previously.[15] Post-labeled PCR products were electrophoresed by using an ABI Prism 310 Genetic Analyzer (PE Applied Biosystems, Foster City, CA) at 30°C.

Dot Blot Hybridization

Primers for PCR were 5′-TGTGGCAGGCCATGCTTCTCG-3′ and 5′-CCCCCTCGGGTGGAAGGAACC-3′ for exon 9, and 5′-GGGCATCGCAGGGTTTCTGAC-

From the *Third Department of Internal Medicine, Hiroshima University School of Medicine, Hiroshima; †Department of Neurology, Tokyo Metropolitan Neurological Hospital, Tokyo; ‡Department of Neurology, Utano National Hospital, Kyoto; and §Department of Neurology, Sumitomo Hospital, Osaka, Japan.

Received Aug 23, 1999, and in revised form Nov 22. Accepted for publication Nov 23, 1999.

Address correspondence to Dr Kawakami, Third Department of Internal Medicine, Hiroshima University School of Medicine, 1-2-3 Kasumi, Minami-ku, Hiroshima 734-8551, Japan.

TA-3′ and 5′-GGCACGGAAAGGTGTAACAGTCG-3′ for exon 15. PCR products (2 μl) were transferred to Gene Screen Plus (NEN Life Science, Boston, MA) and fixed by baking for 1 hour at 80°C. We used sequence-specific oligonucleotide probes that corresponded to the sequence of wild types and variants. The sequences of sequence-specific oligonucleotide probes for wild types were 5′-TCT-GTCCTCAGCCTGGGC-3′ (exon 9) and 5′-AAGTC-ATCCTGCAATGGG-3′ (exon 15), and those for the variants were 5′-TCTGTCCTCGGCCTGGGC-3′ (exon 9) and 5′-AAGTCATCCCGCAATGGG-3′ (exon 15). Membranes were hybridized in tetramethylammonium chloride buffer consisting of 3 M tetramethylammonium chloride, 5 × Denhardt's solution, and 0.1% sodium dodecyl sulfate for 1 hour at 54°C, and were washed at 58°C.

Statistical Analysis

Statistical analysis was performed by using the χ^2 test by JMP software (SAS Institute, Cary, NC), and differences at $p < 0.05$ were considered significant.

Results

We selected randomly 24 subjects from the PD group and performed direct sequence analysis for all the 14 exons in the coding region of the DAT gene, excluding exon 1 that exists in the noncoding region. Direct sequence of the exon 9 fragment revealed an A→G transition at nucleotide 1215 (1215A/G) (the translation starting site in cDNA of the DAT gene is designated as +1), and that of the exon 15 fragment revealed a T→C transition at nucleotide 1898 (1898T/C) (Fig). Both transitions were single-nucleotide polymorphisms (SNPs). However, these SNPs caused no amino acid substitutions.

To identify further polymorphisms, we performed CE-SSCP analysis for 24 subjects also selected randomly from the normal control group. Although we detected two polymorphisms, sequencing the PCR products revealed that these polymorphisms were the same as those that we obtained from direct sequence analysis. Totally, we screened 48 subjects and 96 alleles of the DAT gene in PD subjects and controls, and we screened out all major polymorphisms whose allelic frequency was more than 5%, with a significance level of 7.27×10^{-3}. Probably, there is no other polymorphism that contributes mainly to the pathogenesis of PD in all exons of the DAT gene.

We studied the distribution of these two polymorphisms in all of the subjects by using dot blot hybridization analysis with sequence-specific oligonucleotide probes (Table 1). The 1215G in exon 9 was more frequent in the normal control group than in the PD group. χ^2 analysis on the distribution of genotype and allele frequency revealed a significant difference between the PD and normal control groups (genotype: $\chi^2 = 8.82$, $p = 0.0122$; allele: $\chi^2 = 4.14$, $p = 0.0418$; odds ratio = 2.07; 95% confidence interval, 1.15–3.78). In addition, 1898C in exon 15 was also more frequent in normal controls than in the patient group, but no significant difference existed between the two groups (genotype: $\chi^2 = 1.83$, $p = 0.401$; allele: $\chi^2 = 1.04$, $p = 0.307$; odds ratio = 1.44; 95% confidence interval, 0.788–2.65). Otherwise, a significant positive correlation was observed between 1215G and 1898C in both groups (Table 2).

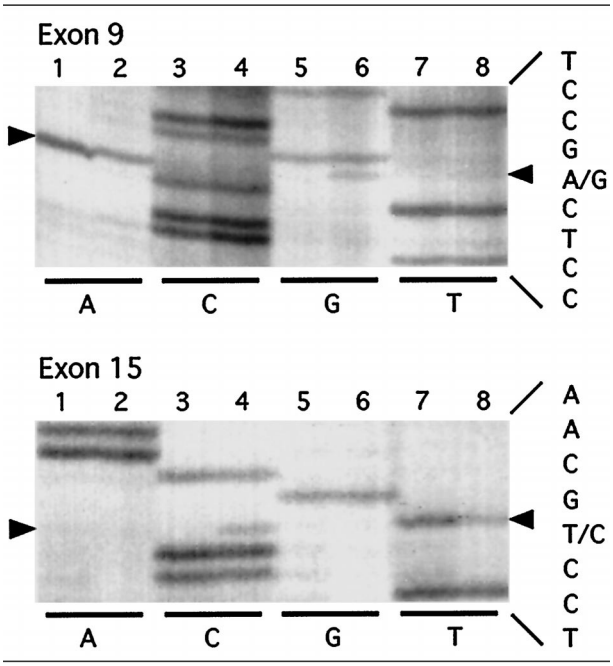

Fig. Direct sequence analysis of exon 9 (top) and that of exon 15 (bottom). Odd and even lanes are subjects without variant and with variant, respectively. Nucleotide transitions (arrowheads) *exist at position 1215 in exon 9 and at position 1898 in exon 15. Because both are in the heterozygous state, the bands at the polymorphisms have only half density (half intensity).*

Discussion

In the present study, we screened the polymorphisms out of the entire coding region of the DAT gene and compared the differences in their distribution between patients with PD and normal controls. Our results indicate that there are two polymorphisms in all the exons of the DAT gene and that one (1215G) is significantly more frequent in the controls than in the patients with PD. The results suggest that 1215G is associated with decreasing the susceptibility to PD.

Previous studies reported that polymorphism of the DAT gene was not associated with PD.[16,17] However, these studies examined only a variable number of tandem repeat polymorphisms in the 3′-untranslated region, and these did not cover exonal polymorphisms. The exonal polymorphisms will be more related to the function of the gene and more conservative than a variable number of tandem repeats in the untranslated re-

Table 1. Frequency of the DAT Gene Polymorphisms

	Genotype				Allele		
1215A/G	A/A	A/G	G/G	Total	A	G	Total
PD	149 (86.6)	21 (12.2)	2 (1.2)	172 (100)	319 (92.7)	25 (7.3)	344 (100)
NC	100 (75.8)	32 (24.2)	0 (0)	132 (100)	232 (87.9)	32 (12.1)	264 (100)
	$\chi^2 = 8.82$	$p = 0.0122$			$\chi^2 = 4.14$	$p = 0.0418$	
1898T/C	T/T	T/C	C/C	Total	T	C	Total
PD	147 (85.4)	23 (13.4)	2 (1.2)	172 (100)	317 (92.2)	27 (7.8)	344 (100)
NC	106 (80.3)	25 (18.9)	1 (0.8)	132 (100)	237 (89.8)	27 (10.2)	264 (100)
	$\chi^2 = 1.83$	$p = 0.401$			$\chi^2 = 1.04$	$p = 0.307$	

Percentages are in parentheses.

DAT = dopamine transporter; PD = Parkinson's disease; NC = normal control.

gion. Therefore, investigation of exonal polymorphisms in this gene might lead to determination of their contribution to PD. Furthermore, polymorphisms of the cytochrome P-450 CYP2D6 gene[4] and glutathione transferase gene[5] have been investigated in recent studies. Polymorphisms of the cytochrome P-450 CYP2D6 gene were reported to be associated with PD at first, but this notion was not reproduced by all groups. Although the studies on these genes suggest that toxic factors contribute to the development of PD, such a genetic predisposition cannot fully explain the mechanism for selective neurodegeneration.

At the beginning, we assumed that nucleotide variations with amino acid substitutions might cause a change in the protein functions of DAT. However, we found only two polymorphisms in all coding regions, and they caused no amino acid substitutions. In this sense, DAT is much conserved in both the nucleotide and the protein levels. If 1215G was associated with development of PD, there would be a mechanism other than one using the protein function of DAT. Therefore, a few possibilities could be suggested. The first possibility is that 1215G would link to the polymorphisms of other genes near the locus. The second and most likely possibility is that the polymorphisms in other regions of the DAT gene would link to 1215G and might decrease the expression level of DAT mRNA. The lowered expression of DAT mRNA might decrease the uptake of toxic factors via DAT and prevent the degeneration of dopaminergic neurons. In fact, the angiotensinogen gene has two mutations, and these mutations are linked to each other.[18] The mutation in the 5′-flanking region affects the basal transcription rate of the angiotensinogen gene and contributes to essential hypertension.

However, our study needs some cautionary notes. First, we enrolled subjects from an ethnic population. Second, our patients were diagnosed as having PD only clinically. All those in the PD group will not have idiopathic PD despite careful clinical selection.[19] Therefore, further and larger studies that recruit subjects from other ethnic populations or patients diagnosed pathologically would reveal a more obvious relationship between DAT and PD, and clarify the mechanism that would explain how the DAT gene contributes to the pathogenesis of PD.

In conclusion, we found two polymorphisms in the exons of the DAT gene, and one of them was associated with decreasing the susceptibility to PD. The investigation on the transporter-based mechanism might explain selective cell loss of dopaminergic neurons in PD and provide a new clue for the prevention of the disease.

Table 2. Disequilibrium between 1215A/G and 1898T/C

PD	1215A/G				NC	1215A/G			
1898T/C	A/A	A/G	G/G	Total	1898T/C	A/A	A/G	G/G	Total
T/T	144	3	0	147	T/T	98	8	0	106
T/C	5	18	0	23	T/C	2	23	0	25
C/C	0	0	2	2	C/C	0	1	0	1
Total	149	21	2	172	Total	100	32	0	132
	$\chi^2 = 280$	$p < 10^{-4}$				$\chi^2 = 81.7$	$p < 10^{-4}$		

PD = Parkinson's disease; NC = normal control.

This study was supported by Grants-in-Aid from the Ministry of Education, Science, and Culture and from the Ministry of Health and Welfare of Japan.

We thank Drs Kenshi Hayashi and Masakazu Inazuka of Kyushu University of Japan for technical advice with CE-SSCP analysis, and acknowledge the contribution of Yasuko Furuno and Hiroko Oguni for their technical assistance.

References

1. Tanner CM, Ottman R, Goldman SM, et al. Parkinson disease in twins: an etiologic study. JAMA 1999;281:341–346
2. Piccini P, Burn DJ, Ceravolo R, et al. The role of inheritance in sporadic Parkinson's disease: evidence from a longitudinal study of dopaminergic function in twins. Ann Neurol 1999;45: 577–582
3. Warner TT, Schapira AH. The role of the alpha-synuclein gene mutation in patients with sporadic Parkinson's disease in the United Kingdom. J Neurol Neurosurg Psychiatry 1998;65: 378–379
4. Smith CA, Gough AC, Leigh PN, et al. Debrisoquine hydroxylase gene polymorphism and susceptibility to Parkinson's disease. Lancet 1992;339:1375–1377
5. Menegon A, Board PG, Blackburn AC, et al. Parkinson's disease, pesticides, and glutathione transferase polymorphisms. Lancet 1998;352:1344–1346
6. Jonsson G, Sachs C. On the mode of action of 6-hydroxydopamine. In: Jonsson G, Molmfors T, Sachs C, eds. Chemical tools in catecholamine research, vol I. Amsterdam: North-Holland, 1975:41–50
7. Burns RS, Chiueh CC, Markey SP, et al. A primate model of parkinsonism: selective destruction of dopaminergic neurons in the pars compacta of the substantia nigra by *N*-methyl-4-phenyl-1,2,3,6-tetrahydropyridine. Proc Natl Acad Sci USA 1983;80:4546–4550
8. Jellinger K. Overview of morphological changes in Parkinson's disease. Adv Neurol 1986;45:1–18
9. Cerruti C, Walther DM, Kuhar MJ, et al. Dopamine transporter mRNA expression is intense in rat midbrain neurons and modest outside midbrain. Mol Brain Res 1993;18:181–186
10. Uhl GR, Walther D, Mash D, et al. Dopamine transporter messenger RNA in Parkinson's disease and control substantia nigra neurons. Ann Neurol 1994;35:494–498
11. Kitayama S, Wang JB, Uhl GR. Dopamine transporter mutants selectively enhance MPP^+ transport. Synapse 1993;15:58–62
12. Kawarai T, Kawakami H, Yamamura Y, et al. Structure and organization of the gene encoding human dopamine transporter. Gene 1997;195:11–18
13. Calne DB, Snow BJ, Lee C. Criteria for diagnosing Parkinson's disease. Ann Neurol 1992;32:S125–S127
14. Sambrooke J, Fritsch EF, Maniatis T. Molecular cloning: a laboratory manual. 2nd ed. Cold Spring Harbor, NY: Cold Spring Harbor Laboratory Press, 1989
15. Inazuka M, Wenz HM, Sakabe M, et al. A streamlined mutation detection system: multicolor post-PCR fluorescence labeling and single-strand conformational polymorphism analysis by capillary electrophoresis. Genome Res 1997;7:1094–1103
16. Higuchi S, Muramatsu T, Arai H, et al. Polymorphisms of dopamine receptor and transporter genes and Parkinson's disease. J Neural Transm Park Dis Dement Sect 1995;10:107–113
17. Plante-Bordeneuve V, Taussig D, Thomas F, et al. Evaluation of four candidate genes encoding proteins of the dopamine pathway in familial and sporadic Parkinson's disease: evidence for association of a DRD2 allele. Neurology 1997;48:1589–1593
18. Inoue I, Nakajima T, Williams CS, et al. A nucleotide substitution in the promoter of human angiotensinogen is associated with essential hypertension and affects basal transcription in vitro. J Clin Invest 1997;99:1786–1797
19. Hughes AJ, Daniel SE, Kilford L, et al. Accuracy of clinical diagnosis of idiopathic Parkinson's disease: a clinico-pathological study of 100 cases. J Neurol Neurosurg Psychiatry 1992;55: 181–184

A Novel Congenital Myopathy with Apoptotic Changes

Koji Ikezoe, MD,*† Chuanzhu Yan, MD,*
Takashi Momoi, PhD,‡ Chikako Imoto, MD,*
Narihiro Minami, PhD,* Masamichi Ariga, MD,§
Kenji Nihei, MD,§ and Ikuya Nonaka, MD*

We report on a female child with congenital myopathy with delayed developmental milestones and mental retardation. The most striking pathological finding was the presence of many condensed to fragmented myonuclei. DNA fragmentation was confirmed by the TUNEL method and supported by the ultrastructural characteristics of apoptotic nuclear changes. We also demonstrated immunohistochemically the activation of caspase-3 and caspase-9. This appears to be the first reported case of congenital myopathy with apoptotic process.

Ikezoe K, Yan C, Momoi T, Imoto C, Minami N, Ariga M, Nihei K, Nonaka I. A novel congenital myopathy with apoptotic changes. Ann Neurol 2000;47:531–536

Congenital myopathies constitute a group of disorders that show hypotonia and weakness at birth or in early childhood. They are accompanied by delayed developmental milestones and dysmorphic features such as high-arched palate, elongated face, and joint contractures. The major congenital myopathies have been classified on the basis of the following characteristic structural abnormalities: central core disease,[1] nemaline

From the Departments of *Ultrastructural Research and ‡Development and Differentiation, National Institute of Neuroscience, National Center of Neurology and Psychiatry, and §Department of Neurology, National Children's Hospital, Tokyo; and †Department of Neurology, Neurological Institute, Faculty of Medicine, Kyushu University, Fukuoka, Japan.

Received Aug 9, 1999, and in revised form Nov 9. Accepted for publication Dec 2, 1999.

Address correspondence to Dr Ikezoe, Department of Ultrastructural Research, National Institute of Neuroscience, National Center of Neurology and Psychiatry, Tokyo 187-8502, Japan.

myopathy,[2] myotubular myopathy,[3] and congenital fiber-type disproportion. However, many patients remain with the clinical characteristics of congenital myopathy with nonspecific diagnostic morphological features.

Apoptosis, originally defined by morphological changes mainly in the nuclei,[4] is an active cell death under genetic control. Many apoptotic signaling pathways have been identified. Many of them require the sequential activation of caspases, the final step of which is the activation of caspase-3. Activated caspase-3 processes the inhibitor of caspase-activated DNase (ICAD), which results in activation of the caspase-activated DNase (CAD) that causes DNA fragmentation.[5] Caspase-9, which is upstream of caspase-3, is activated by cytochrome *c*/apoptotic protease-activating factor-1 (Apaf-1); cytochrome *c* released from mitochondria binds to Apaf-1 and then activates caspase-9.[6]

The release of cytochrome *c* is inhibited by Bcl-2, and Bax functions conversely.[7] The apoptotic process is involved in many diseases including cancers, autoimmune diseases, neurodegenerative diseases, and other pathological conditions. Several muscle diseases are also reported to be related to apoptosis, but whether they are is still being debated.[8–11]

We report a patient with an unusual congenital myopathy with pronounced myonuclear changes on light microscopic examination. To determine whether an apoptotic process was involved in this case, we examined muscle sampled for biopsy by electron microscopy, by the terminal deoxynucleotidyl transferase (TdT)-mediated dUTP nick end-labeling (TUNEL) method, and by immunohistochemistry. The results strongly support the presence of apoptotic degeneration in our patient.

Patient and Methods

Patient

A 4-year-old girl was born at full term after an uneventful pregnancy and delivery. Her parents were healthy and nonconsanguineous. At birth, she was floppy and her head circumference measured 29.5 cm (−2.8 cm SD).

Her psychomotor development was markedly delayed. She obtained head control at 6 months; however, she could neither sit alone nor speak meaningful words by 3 years of age.

On examination at the age of 3 years, her height, weight, and head circumference were 90 cm (−0.6 cm SD), 7.5 kg (−4.0 kg SD), and 38 cm (−6.4 cm SD), respectively. Her face was myopathic with an open bite, and her palate was high arched. She had bilateral ankle joint contractures and equinovarus.

There were no signs of cranial nerve involvement except facial weakness and dysphagia. She showed no obvious cerebellar ataxia. No ocular abnormalities, including cataracts, were noted. She had moderate generalized muscle atrophy, weakness, and hypotonia but no calf hypertrophy. Tendon reflexes were absent with no pathological reflexes. There was no history of respiratory difficulties or cardiomyopathy. She had not been treated with corticosteroids.

The concentration of serum creatine kinase was 148 IU/L (normal, <200 IU/L). Concentrations of serum aldolase, pyruvate, and lactate were also normal. Needle electromyography showed myopathic changes in the limbs. Her head magnetic resonance imaging scan showed no abnormalities. There were no cardiac abnormalities on the ultrasonographic cardiogram.

A biopsy of the left biceps brachii was performed when she was 3 years 2 months of age.

Methods

One portion of the biopsy specimen was frozen in isopentane cooled in liquid nitrogen. Serial frozen sections were stained with hematoxylin and eosin, modified Gomori trichrome, and by various histochemical methods. Another portion was processed for electron microscopy.

For the TUNEL method, we used an in situ apoptosis detection kit (Takara shuzo, Otsu, Japan) on frozen sections. TUNEL-positive nuclei were visualized with diaminobenzidine.

For immunohistochemistry, the primary antibodies, monoclonal anti-Bcl-2 (1:40; Dako, Denmark) and polyclonal anti-Bax (1:30; Calbiochem, Cambridge, MA) were treated with peroxidase-labeled secondary antibodies and visualized with DAB; monoclonal anti-dystrophin C terminus (1:100; Novocastra, Newcastle, UK), anti-α-sarcoglycan (1:50; Novocastra), anti-α-dystroglycan (1:50; Upstate,), anti-β-dystroglycan (1:100; Novocastra), and anti-merosin (1:500; Chemicon) were treated with FITC–labeled secondary antibodies and examined by fluorescence microscopy. In addition, we examined the activation of caspase-3 and caspase-9 with antibodies against them (anti-activated caspase-3 and caspase-9 antibodies, 1:250 and 1:100, respectively). These were rabbit affinity-purified polyclonal antibodies raised against the pentapeptide of the human caspase-3 cleavage site GIETD[12] and the human caspase-9 cleavage site FDQLD (Momoi T and colleagues, unpublished data), respectively. We also used nonimmune rabbit serum as a negative control for these antibodies.

We compared the results of TUNEL and immunohistochemistry with five age-matched control muscle biopsies with nondiagnostic findings.

Results

On light microscopy, most muscle fibers were small with fiber-size variation averaging 15 μm in diameter, with mild interstitial fibrosis and many basophilic fibers, but few necrotic fibers. There was no inflammation. Many fibers had high acid phosphatase activity (Fig 1D), and several fibers had cytoplasmic bodies and sarcoplasmic masses. On ATPase stain, types 1, 2A, 2B, and 2C fibers comprised 42%, 11%, 7%, and 40%, respectively. About 20% of fibers had vacuoles (see Fig 1B) and, occasionally, rimmed vacuoles. In addition, myonuclear alterations that consisted of chromatin condensation, occasionally associated with nuclear fragmentation, were seen (see Fig 1A).

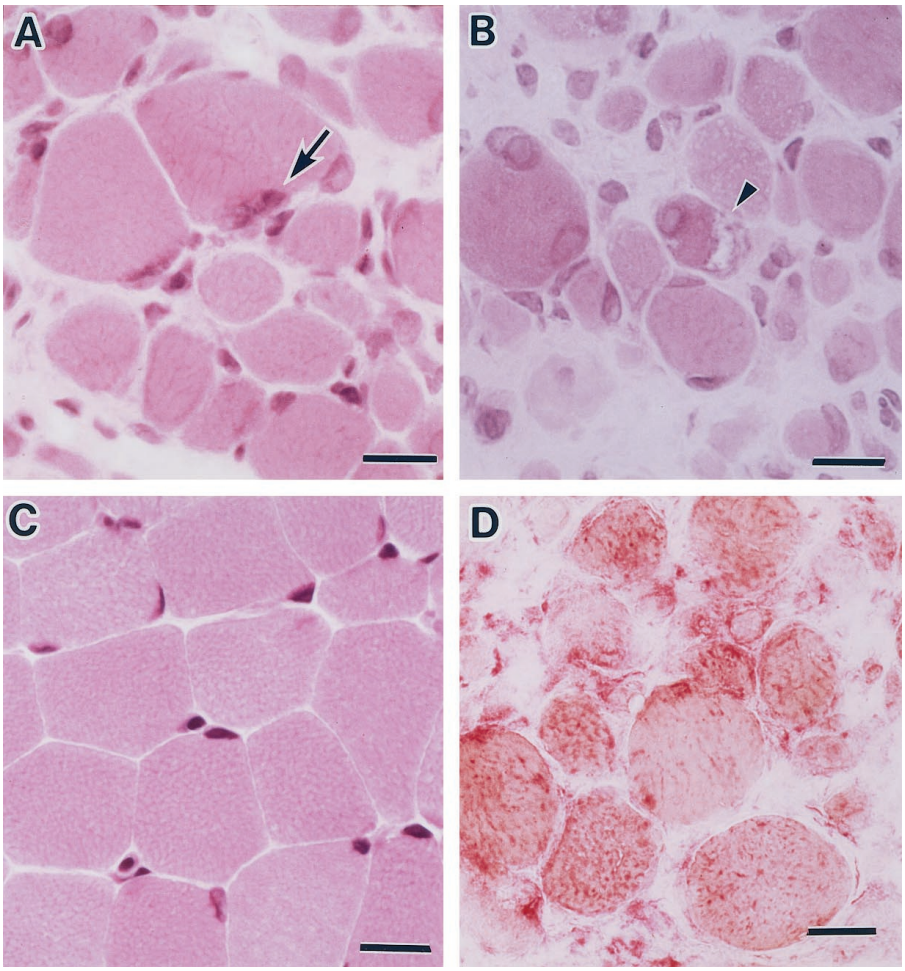

Fig 1. Light microscopic findings in this patient (A, B, and D) and age-matched control muscle (C). (A) In addition to variation in fiber size and interstitial fibrosis, myonuclear alterations with chromatin condensation and fragmentation (arrow) *are conspicuous. (B) Vacuoles* (arrowhead) *are also seen. (D) Many fibers show high acid phosphatase activity. Hematoxylin and eosin (A, B, and C); acid phosphatase (D). Scale bars = 20 μm (A–D).*

On electron microscopy, approximately 40% of myonuclei had abnormal morphologies. The most common change was condensation of chromatin granules (Fig 2A). In the more degenerated myonuclei, the nuclear membrane was indented, and the nucleoplasm was filled with autophagic vacuoles and myeloid bodies (see Fig 2B). Finally, degenerated myonuclei were fragmented (see Fig 2C). In the muscle fibers with degenerated myonuclei, myofibrils were disorganized, especially in the vicinity of the myonuclei, and numerous autophagic vacuoles and myeloid bodies were seen (see Fig 2D). There were no typical apoptotic bodies.

The TUNEL method revealed that 2% of myonuclei in nonnecrotic fibers were positively stained (Fig 3A and B). None of the normal controls had TUNEL-positive myonuclei.

Bcl-2 was not expressed in muscle fibers. On the other hand, Bax-positive fibers constituted over 80% (see Fig 3C and E). In control muscles, we detected weak expression of Bcl-2 and no expression of Bax (see Fig 3D and F).

The most striking finding was expression of activated caspase-3 and caspase-9. About 6% of fibers expressed the former, and about 1% expressed the latter. All fibers with activated caspase-9 reaction highly expressed activated caspase-3 activity (see Fig 3G and H), but there were no fibers in which the activated caspase-3 reaction and TUNEL-positive myonuclei coexisted. In control muscles, activated caspases were not found.

Immunoreactivities to anti-dystrophin, α-sarcoglycan, α-dystroglycan, β-dystroglycan, and merosin antibodies were all positive, similar to normal controls.

Discussion

It has been reported that apoptotic processes are involved in Duchenne muscular dystrophy,[8] limb-girdle muscular dystrophy type 2A,[9] and Marinesco-Sjögren syndrome.[10] In addition, distal myopathy with rimmed vacuoles is also thought to be a possible member of the class of diseases with apoptosis.[13,14] Clinically, this patient's findings differed from these diseases. Moreover, she showed normal dystrophin expression, no mutation of the calpain-3 gene (data not shown), and no cataracts or cerebellar signs characteristic of the Marinesco-Sjögren syndrome. Among these diseases, Marinesco-

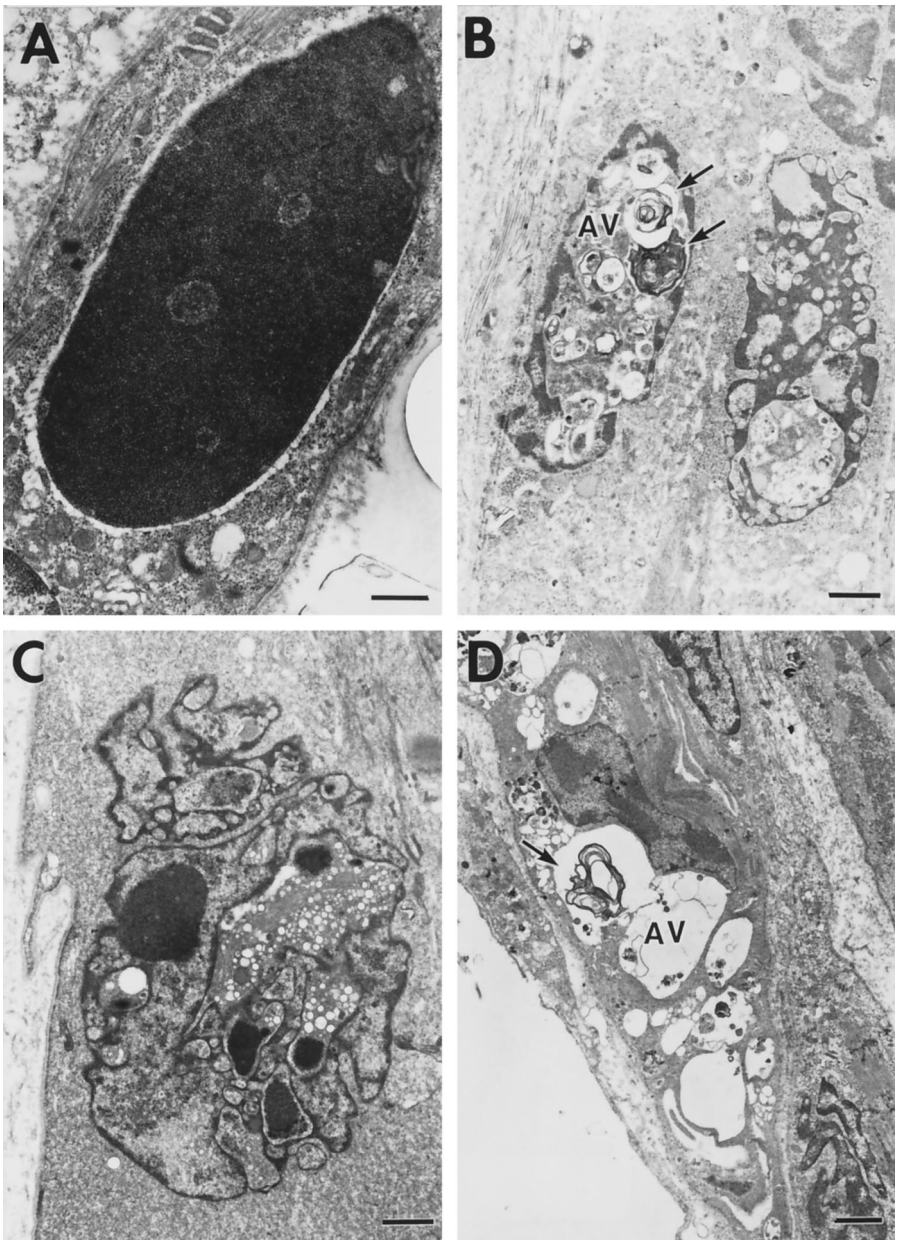

Fig 2. Electron microscopic findings. (A) A myonucleus that shows marked condensation of chromatin granules. This is the typical myonuclear alteration seen in this patient. (B) In a more advanced stage, degenerated myonuclei show indentations and are occasionally filled with autophagic vacuoles (AV) *and myeloid bodies* (arrow). *(C) The nuclear membrane of this myonucleus is deeply indented, resulting in the fragmentation of condensed chromatin and nucleoplasm. (D) In degenerated muscle fibers, there are many autophagic vacuoles* (AV) *and myeloid bodies* (arrow), *especially in the vicinity of the altered myonuclei. Scale bars = 0.5 μm (A), 1 μm (B and C), and 2 μm (D).*

Sjögren syndrome and distal myopathy with rimmed vacuoles show little necrosis and regeneration. Our patient showed the following several pathological findings in common with these two diseases: (1) DNA fragmentation in myonuclei demonstrated by the TUNEL method, (2) condensation and marginalization of the chromatin in myonuclei on electron microscopy, (3) myofibrillar degeneration in the fibers with abnormal myonuclei, and (4) rimmed or nonrimmed vacuole formation and a paucity of necrotic and regenerating processes. These findings suggest that this patient shares a pathogenetic mechanism that leads to muscle fiber degeneration in common with these two diseases.

As a rule, cells involved in apoptosis finally form apoptotic bodies; ie, fragments of the degraded apoptotic cell are enclosed by a cell membrane and phagocytosed by macrophages or neighboring cells.[15] However, there were no visible apoptotic bodies in this patient. The muscle cell is a multinucleated cell, and it is unlikely that all the nuclei in a cell undergo apoptosis. Instead, a single or a limited number of myonuclei scattered throughout the cell may undergo apoptosis independently.[9] Therefore, apoptosis does not occur throughout a long muscle cell but does so focally or segmentally with myofibrillar degeneration around the apoptotic myonuclei. Although the cause of myofibrillar degeneration in this patient is unknown, it may have been initiated by activated caspases that have the capacity

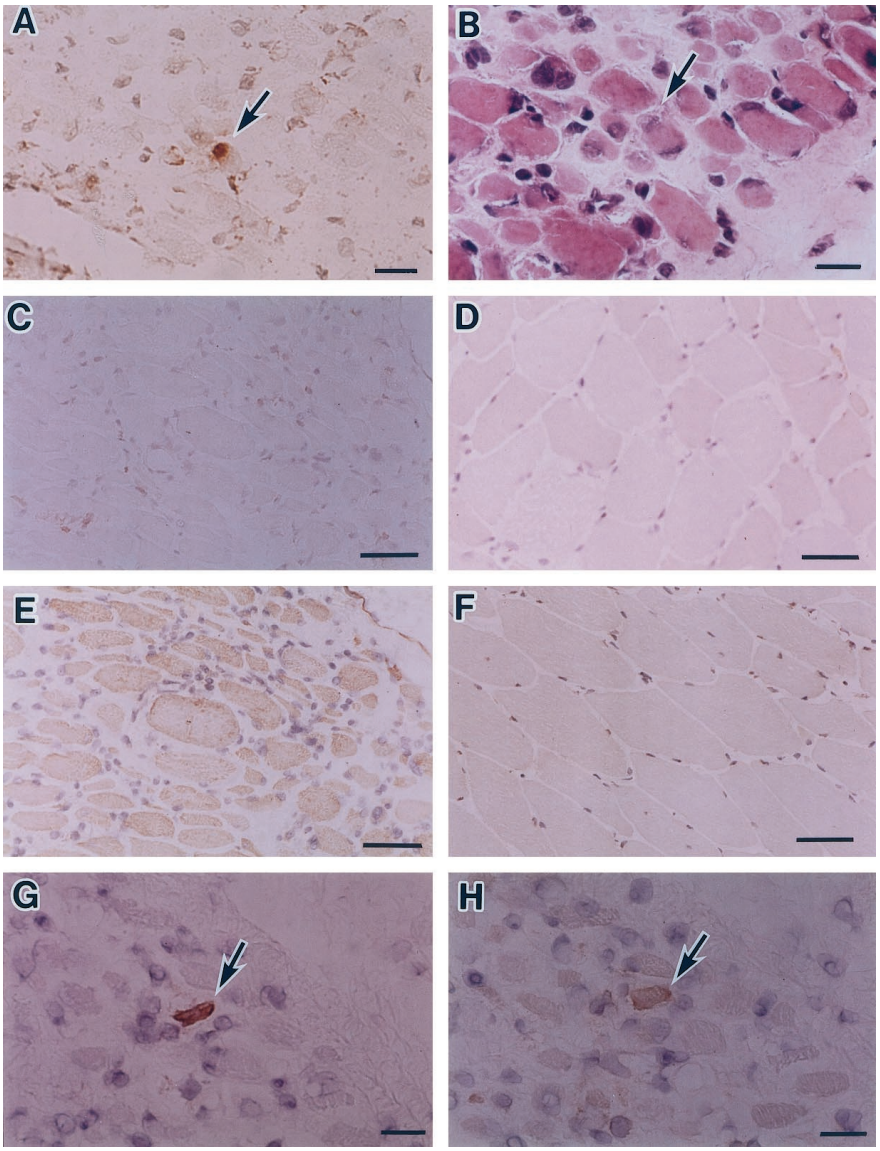

Fig 3. A TUNEL-positive myonucleus (A and B), and Bcl-2 (C), Bax (E), activated caspase-9 (G), and activated caspase-3 (H) immunohistochemical stains in this patient, and immunohistochemical stains of Bcl-2 (D) and Bax (F) in age-matched control muscles. (A) There is a TUNEL-positive myonucleus (arrow) *in a nonnecrotic muscle fiber. (B) The TUNEL-positive myonucleus in A is shown in this serial section* (arrow). *(C) No muscle fibers express anti-apoptotic Bcl-2 in this patient. (D) Almost all type 2A and 2B fibers have weak expression of anti-apoptotic Bcl-2 in control muscles. (E) In contrast to Bcl-2, most fibers express pro-apoptotic Bax in this serial section of C. (F) In control muscles, no muscle fibers express pro-apoptotic Bax. (G) About 1% of muscle fibers express the activated caspase-9 activity* (arrow). *(H) Activated caspase-3 activity is found in 6% of fibers. Note that in this serial section of E, the same fiber also expresses activated caspase-3* (arrow). *Without exception, fibers with activated caspase-9 show activated caspase-3 activity. TUNEL method, diaminobenzidine (A); hematoxylin and eosin (B); diaminobenzidine, lightly counterstained with hematoxylin (C–H). Scale bars = 20 μm (A, B, G, and H) and 50 μm (C, D, E, and F).*

to cleave actin,[16] and calpains,[17,18] which are subsequently processed by proteasomes.[17]

Finally, only focally degraded cellular debris in a muscle cell is removed and, therefore, no apoptotic bodies are formed.

In this patient, although we detected 40% of abnormal myonuclei, mainly showing chromatin condensation, only 2% of myonuclei were TUNEL positive. This may reflect a difference in the molecules that carry out chromatin condensation and DNA fragmentation. For example, apoptosis-inducing factor causes chromatin condensation but fragments DNA into nucleosome size.[19] We demonstrated immunohistochemically the activation of caspase-9 and the subsequent caspase-3 activation in the same fibers. In this patient, down-regulation of Bcl-2 expression, which is weakly expressed in type 2 fibers in normal muscle,[20] and up-regulation of Bax, which shows no expression in normal muscle, may also reflect the proposed apoptotic process. We could not find activated caspase-3– and TUNEL-positive myonuclei in the same fibers, perhaps because the apoptotic signaling process occurred too rapidly.

In conclusion, this morphological study strongly suggests that apoptotic mechanisms play a role in the pathogenesis of this newly recognized congenital myopathy.

We thank Prof S. M. Sumi (University of Washington, Seattle, WA) for his kind review of this study. We also greatly appreciate the technical assistance of Drs Y. Kozuka, Y. Saito, and M. Nakagawa and Miss F. Igarashi.

References

1. Shy GM, Magee KR. A new congenital non-progressive myopathy. Brain 1956;79:610–621
2. Shy GM, Engel WK, Somers JE. Nemaline myopathy: a new congenital myopathy. Brain 1963;86:793–810
3. Spiro AJ, Shy GM, Gonatas NK. Myotubular myopathy: persistence of fetal muscle in an adolescent boy. Arch Neurol 1966;14:1–14
4. Kerr JFR, Wyllie AH, Currie AR. Apoptosis: a basic biological phenomenon with wide-range implications in tissue kinetics. Br J Cancer 1972;26:239–257
5. Sakahira A, Enari M, Nagata S. Cleavage of CAD inhibitor in CAD activation and DNA degradation during apoptosis. Nature 1998;391:96–99
6. Liu X, Kim CN, Yang J, et al. Induction of apoptotic program in cell-free extracts: requirement for dATP and cytochrome c. Cell 1996;86:147–157
7. Oltvia ZN, Korsmeyer SJ. Checkpoints of dueling dimers foil death wishes. Cell 1994;79:189–192
8. Sandri M, Minetti C, Pedemonte M, Carraro U. Apoptotic myonuclei in human Duchenne muscular dystrophy. Lab Invest 1998;78:1005–1016
9. Baghdiguian S, Martin M, Richard I, et al. Calpain 3 deficiency is associated with myonuclear apoptosis and profound perturbation of the IκBα/NF-κB pathway in limb-girdle muscular dystrophy type 2A. Nat Med 1999;5:503–511
10. Suzuki Y, Murakami N, Goto Y, et al. Apoptotic nuclear degeneration in Marinesco-Sjögren syndrome. Acta Neuropathol 1997;94:410–415
11. Olive M, Martinez-Matos JA, Montero J, Ferrer I. Apoptosis is not mechanism of cell death of muscle fibers in human muscular dystrophies and inflammatory myopathies. Muscle Nerve 1997;20:1328–1330
12. Kouroku Y, Urase K, Fujita E, et al. Detection of activated caspase-3 by a cleavage site-directed antiserum during naturally occurring DRG neurons apoptosis. Biochem Biophys Res Commun 1998;247:780–784
13. Nonaka I, Murakami N, Suzuki Y, Satoyoshi E. Nuclear degeneration and rimmed vacuole formation in neuromuscular disorders. In: Askanas V, Serratrice G, Engel WK, eds. Inclusion-body myositis and myopathies. Cambridge: Cambridge University Press, 1998:297–305
14. Nonaka I, Murakami N, Suzuki Y, Kawai M. Distal myopathy with rimmed vacuoles. Neuromusc Disord 1998;8:333–337
15. Ruff M. Cell suicide for beginners. Nature 1998;396:119–122
16. Mashima T, Naito M, Noguchi K, et al. Actin cleavage by CPP-32/apopain during the development of apoptosis. Oncogene 1997;14:1007–1012
17. Kumamoto T, Fujimoto S, Nagao S, et al. Proteasomes in distal myopathy with rimmed vacuoles. Intern Med 1998;37:746–752
18. Wood DE, Newcomb EW. Caspase-dependent activation of calpain during drug-induced apoptosis. J Biol Chem 1999;274:8309–8315
19. Zamzami N, Kroemer G. Condensed matter in cell death. Nature 1999;401:127–128
20. Ibi T, Sahashi K, Jing L, et al. Immunostaining of anti-Bcl-2 antibody in diseased human muscles. Clin Neurol (Tokyo) 1996;36:735–740

Novel Missense Mutations in the Glycogen-Branching Enzyme Gene in Adult Polyglucosan Body Disease

Focke Ziemssen, BS,* Eckhart Sindern, MD,* J. Michael Schröder, MD,† Yoon S. Shin, MD,‡ Jahen Zange, PhD,§ Manfred W. Kilimann, MD,‖ Jean-Pierre Malin, MD,* and Matthias Vorgerd, MD*

We describe the first non-Ashkenazi patient with adult polyglucosan body disease and decreased glycogen-branching enzyme (GBE) activity in leukocytes. Gene analysis revealed compound heterozygosity for two novel missense mutations Arg515His and Arg524Gln in the GBE gene. Both missense mutations are predicted to impair GBE activity. This is the first identification of GBE mutations underlying adult polyglucosan body disease in a non-Ashkenazi family, and confirms that adult glycogen storage disease type IV can manifest clinically as adult polyglucosan body disease.

Ziemssen F, Sindern E, Schröder JM, Shin YS, Zange J, Kilimann MW, Malin JP, Vorgerd M. Novel missense mutations in the glycogen-branching enzyme gene in adult polyglucosan body disease. Ann Neurol 2000;47:536–540

Adult polyglucosan body disease (APBD) is a rare neurological disease caused by an accumulation of spherical intra-axonal inclusion bodies in the central and peripheral nervous system. Clinical features consist of lower and upper motor neuron signs, dementia, and urinary dysfunction.[1–5] In Ashkenazi-Jewish patients with APBD, glycogen-branching enzyme (GBE) deficiency was documented in leukocytes and peripheral nerve biopsies.[6,7] Similar biochemical findings occur in glycogen storage disease type IV (GSD IV), which, in contrast to APBD, is typically an early childhood disorder with hepatic or multisystemic manifestations.[8,9] The gene of the ubiquitously expressed GBE was a candidate for involvement in APBD, and a homozygous missense mutation in the GBE gene on chromo-

From the *Department of Neurology and ‖Institute for Physiological Chemistry, Ruhr University Bochum, Bochum; †Department of Neuropathology, University of Aachen, Aachen; ‡Department of Pediatrics, University of Munich, Munich; and §Institute of Aerospace Medicine, German Aerospace Center, Cologne, Germany.

Received Sep 8, 1999, and in revised form Dec 2. Accepted for publication Dec 2, 1999.

Address correspondence to Dr Vorgerd, Department of Neurology, Ruhr-University, Kliniken Bergmannsheil, Bürkle-de-la-Camp-Platz 1, 44789 Bochum, Germany.

some 3 (Tyr329Ser) has recently been identified in 7 patients from five Ashkenazi families.[6] However, GBE activity in leukocytes and sural nerve biopsies was normal in several non-Ashkenazi APBD patients.[7] This suggested possible genetic heterogeneity of APBD, or the possibility that an APBD phenotype caused by GBE deficiency might be associated exclusively with the Tyr329Ser mutation, or even that this mutation might only be a polymorphism in close linkage with a causal mutation in another gene.

In the present study, we describe the first non-Ashkenazi patient with APBD and decreased GBE activity. Mutational analysis revealed two novel mutations in the GBE gene, confirming that APBD can be caused by GBE mutations.

Patients and Methods

Patient

A 46-year-old German woman presented with gait disturbance that had progressed for 3 years, urinary urge incontinence, and hearing loss. Neurological examination showed moderate spastic tetraparesis, generalized symmetrical hyperreflexia except for depressed ankle jerks, bilateral extensor plantar response, diminished vibration sensation in the legs, and impaired superficial sensation in a stocky pattern. Magnetic resonance imaging demonstrated confluent areas of hyperintensity on T2-weighted images in the periventricular white matter. Brainstem auditory and somatosensory evoked potentials were impaired bilaterally. Nerve conduction studies and electromyography indicated a sensorimotor peripheral neuropathy with mixed axonal and demyelinating features. Complete neurological and neurophysiological examination of her two symptomatic daughters (ages 14 and 21 years) was normal. Sural nerve biopsy in the patient revealed a neuropathy with an approximately 40% decrease of large myelinated fibers. Occasional clusters of regenerated axons and axons with thin myelin sheaths were observed. Many fibers showed axonal spheroids. Electron microscopy revealed that they were composed of osmiophilic granules and irregular filaments characteristic of polyglucosan bodies (Fig 1). GBE activity in the patient's leukocytes was 20% of the lower limit of the normal range (0.02 nmol/min/mg of protein; normal, 0.1–0.5 nmol/min/mg of protein; n = 40). The two daughters displayed intermediate levels of GBE activity of 80% (0.08 nmol/min/mg of protein) in leukocytes. In the patient's leukocytes, phosphorylase *a* (*a* + *b*) [5.7 (19.3) nmol/min/mg of protein; normal, 5–20 (10–50) nmol/min/mg of protein; n = 40] and glycogen [2.7 mg/dl; normal, 0–10 mg/dl; n = 40] as well as phosphorylase kinase in erythrocytes (218 mmol/min/g of hemoglobin; normal, 100–300 mmol/min/g of hemoglobin; n = 40) were normal. The clinical, biochemical, and neuropathological findings were described in detail in a previous report.[10]

The patient refused a muscle biopsy. However, to analyze a possible muscle involvement in APBD, skeletal muscle energy metabolism in the patient was measured noninvasively by ^{31}P-magnetic resonance spectroscopy according to a standard protocol.[11] Energy metabolism was monitored continuously from the right gastrocnemius muscle at rest, during aerobic and anaerobic isometric muscle contraction at 30% of the force at maximum voluntary contraction for 3 min-

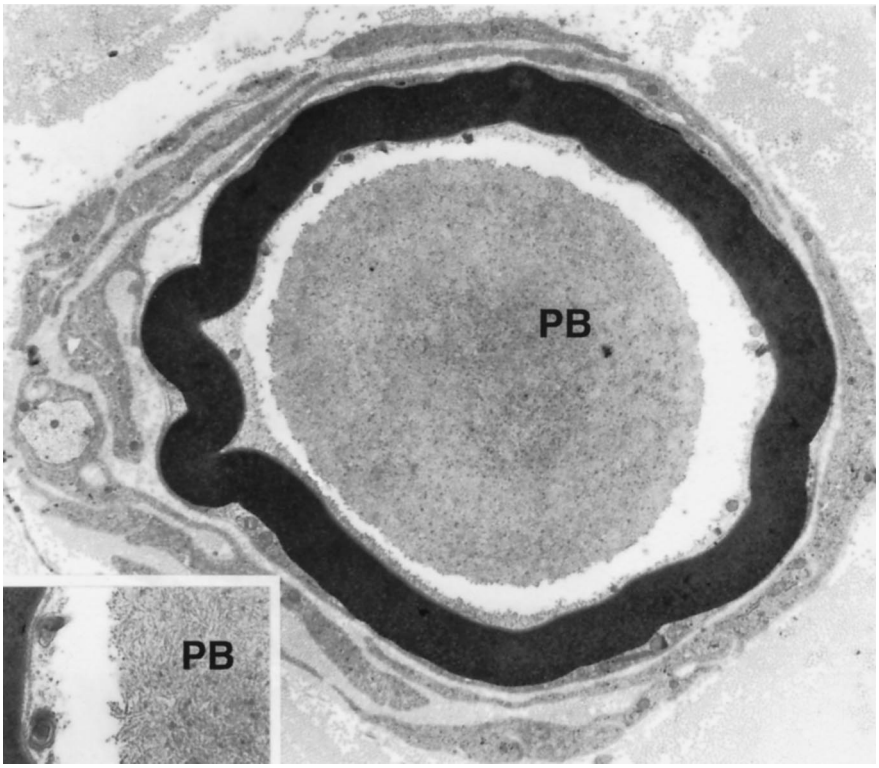

Fig 1. Sural nerve biopsy. Electronmicroscopic view of a large polyglucosan body (PB) *in a thin myelinated nerve fiber surrounded by several Schwann cell processes (incipient onion bulb formation) (magnification, ×9,200 before 16% reduction). High-power view that shows the fine structure of PBs, which appear to include filamentous, granular, and amorphous components (inset; magnification ×27,800 before 16% reduction).*

utes, and during recovery from exercise. Values for the levels of phosphocreatine (PCr), ATP, ADP, inorganic phosphate (Pi), intracellular pH, the rates of [PCr] + [ATP] decrease per force-time integral, and the time constants for PCr recovery after contraction were normal (data not shown). Thus, noninvasive ^{31}P-magnetic resonance spectroscopy indicates normal glycogen metabolism in skeletal muscle.

Mutational Analysis of the GBE Gene

REVERSE TRANSCRIPTION-POLYMERASE CHAIN REACTION. Purification of RNA and genomic DNA from deep-frozen blood samples was performed according to standard procedures. The complete GBE coding sequence was amplified by reverse transcription–polymerase chain reaction (RT–PCR) and analyzed by direct cycle sequencing by using an automated fluorescence sequencer (ABI 377; Perkin-Elmer, Foster City, CA). The following primer pairs deduced from the human cDNA sequence[12] were used to amplify the complete GBE coding sequence in six overlapping fragments: fragment 1: forward primer 1F, 5′-ATTCGGTCCCAGCTAGAGC-3′ and the reverse primer 1R, 5′-TCAGCACATCTGTG-GACGC-3′; fragment 2: 2F, 5′-CATTGGAGAAAATGAAG-GTGG-3′, and 2R, 5′-AAGGCCTTTGATTCTTGGTAG-3′; fragment 3: 3F, 5′-GAGTTTAAGCATTCCAGACC-3′, and 3R, 5′-AGGCAAACAATCTGCTATCC-3′; fragment 4: 4F, 5′-TCATTCTGGACCTAGAGGG-3′, and 4R, 5′-ATGCACTTTTCAAGGTAGCG-3′; fragment 5: 5F, 5′-AG-ATGAAGACTGGAACATGG-3′, and 5R, 5′-ACTCACG-TAGGCCTGTGG-3′; and fragment 6: 6F, 5′-GGAAGAA-AGATATGGTTGGC-3′, and 6R, 5′-AGCTGTGTGAC-AGTGATAAC-3′.

RESTRICTION ENZYME ANALYSIS OF GENOMIC DNA. To confirm the mutations in the patient and to analyze both asymptomatic daughters as well as normal control subjects, PCR of genomic DNA was performed with the forward primer 6A, 5′-CAAACATGAGTGTCCTGACTCC-3′, and the reverse primer 6B, 5′-ACCAAGCCCATGCGT-AATGAG-3′. PCR products were digested with *Bcl*I and *Taq*I and analyzed on a 7.5% polyacrylamide gel with 1 × Tris-borate EDTA (TBE) buffer at 10 V/cm.

Results

Two novel G-to-A transitions in the GBE gene were identified, one at nucleotide 1634 and the other at nucleotide 1661 (nucleotide positions of the cDNA and protein sequence are numbered according to data from Thon and co-workers[12]) (Fig 2). The first mutation is a missense mutation that changes the CGT codon for arginine at amino acid position 515 into a CAT histidine codon (Arg515His). The second is another missense mutation that changes the arginine codon at amino acid position 524 into a CAA glutamine codon (Arg524Gln). The remainder of the coding sequence was identical to that of the wild-type GBE gene. Both mutations are localized within a region of the human GBE coding sequence (codon 512–528) that is identical to the coding sequence of *Saccharomyces cerevisiae*.[12] Both mutations were confirmed by PCR on genomic DNA from the patient, followed by *Bcl*I and *Taq*I digestion (Fig 3B). Restriction enzyme analysis revealed that the asymptomatic daughters with intermediate GBE activity in leukocytes both carry one of the mutations, which thus demonstrates that the two missense mutations were located on different alleles. One was heterozygous for Arg515His and the other heterozygous for Arg524Gln (see Fig 3).

Both missense mutations were shown to be absent in a panel of 50 unrelated German healthy control subjects, which suggests that they are disease-causing mutations and not common polymorphisms.

Discussion

Two novel missense mutations in the GBE gene, Arg515His and Arg524Gln, were identified in the first non-Ashkenazi patient with APBD and GBE deficiency in leukocytes. Two asymptomatic daughters both had intermediate GBE activity in leukocytes and were shown to be heterozygous mutation carriers. We

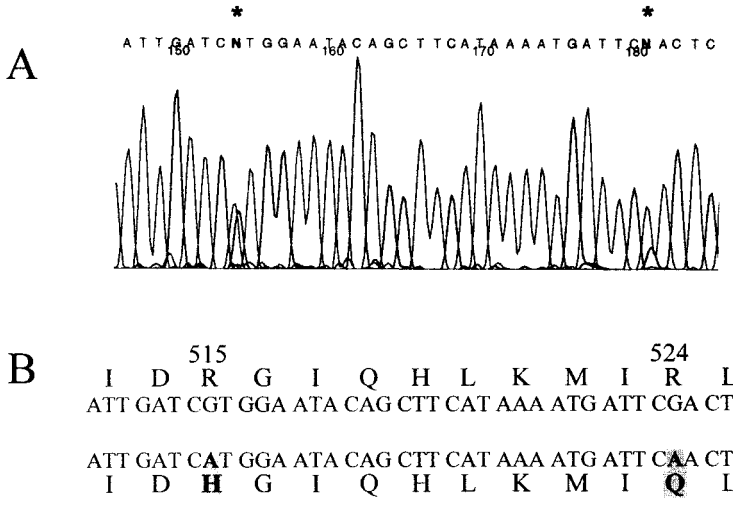

Fig 2. Identification of glycogen-branching enzyme mutations in the patient with adult polyglucosan body disease. (A) Sequencing recordings of patient reverse transcription–polymerase chain reaction product, which documents a G-to-A transition at nucleotide 1634 and a G-to-A transition at nucleotide 1661. Substitutions are indicated by an asterisk. *(B) Wild-type (wt) and mutant sequences are shown in comparison, with mutant* (mut) *sequence positions highlighted.*

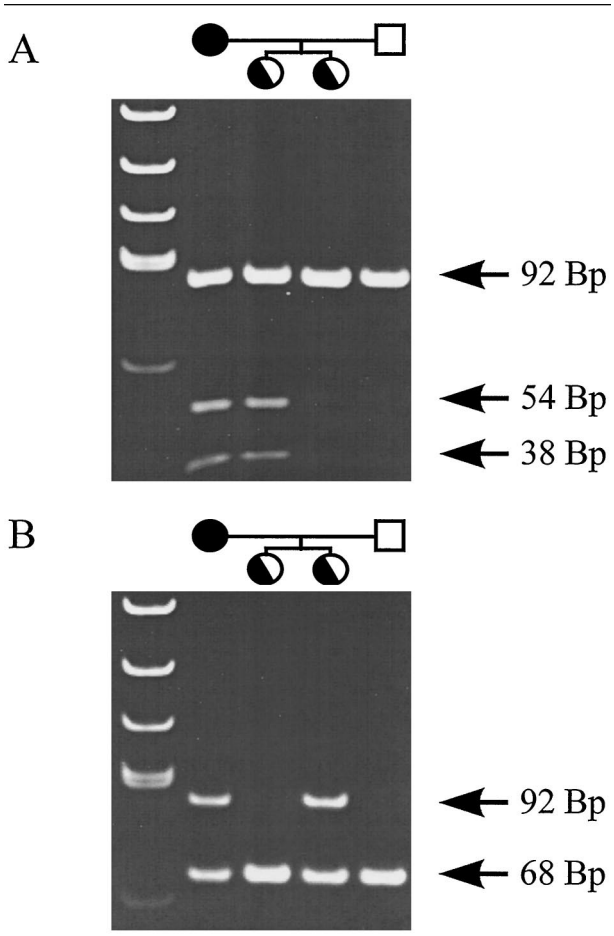

Fig 3 (A) Identification of the G1634A transition by restriction digestion. After restriction digestion by using Bcl*I, the normal allele is not cleaved and yields one 92-bp fragment in the husband and the younger daughter. The mutation at nucleotide 1634 creates a* Bcl*I restriction site, which results in additional 54-bp and 38-bp fragments in the patient and her older daughter. (B) Identification of the G1661A transition by restriction digestion;* Taq*I cleaves the 92-bp fragment completely into 68-bp and 24-bp fragments in the patient's husband and her older daughter. The latter fragment cannot be seen because of its weak signal intensity. The mutation destroys the* Taq*I restriction site, which results in two bands (92 bp and 68 bp) in the patient and her younger daughter. Fragment lengths (Bp) are shown on the right. Digested products were separated on a 7.5% polyacrylamide gel. Lane 1 represents the molecular weight marker (pUC19 DNA/*Msp*I).*

conclude that both substitutions are disease-causing mutations for the following reasons: first, no other alterations were detected in the remaining GBE coding sequence; second, these mutations were not detected in 50 control persons; and, third, the mutations were associated with decreased GBE activity in the asymptomatic daughters of the patient. It is noteworthy that both Arg residues are conserved between the human GBE coding sequence and that of *Saccharomyces cerevisiae*.[12,13]

The present study adds two new mutations to the previously characterized six mutations in the GBE gene (Leu224Pro, Phe257Leu, Tyr329Ser, Arg515Cys, Arg524Stop, 210-bp deletion).[6,14] Our data confirm, for the first non-Ashkenazi family, that APBDs associated with GBE deficiency and GSD IV are allelic disorders encoded by mutations in the same GBE structural gene. Thus, GSD IV occurs in very different clinical presentations—hepatic (M. Andersen) and neuromuscular forms as well as APBD. The molecular mechanisms underlying this pronounced clinical heterogeneity of GSD IV remain enigmatic and have been discussed in detail elsewhere.[6,14] Defects in tissue-specific isoenzymes encoded by different genes expressed in different tissues are unlikely, because there is no clear evidence for the existence of isoenzymes of the GBE. Different isoforms of GBE encoded by one GBE gene might exist that are expressed tissue specifically. Differential sensitivities of the mutant enzyme to proteases or to posttranslational modifications in different cell types and additional genetic or extrinsic factors may also contribute to the heterogeneity of GSD IV. It is noteworthy that codons 515 and 524 of the GBE gene, in the APBD family reported at present, were also mutated in 2 patients with GSD IV (Arg515Cys and Arg524Stop) who had progressive liver cirrhosis and failure.[14] This region may therefore be a mutation hotspot in patients with GSD IV.

A more specific genotype/phenotype relationship in GSD IV may be emerging, although the present number of known mutations is still too low for definitive conclusions. The Jewish patients with APBD, reported by Lossos and co-workers,[6] were homozygous for the Tyr329Ser missense mutation. The non-Jewish patient described here has two different missense mutations in the GBE gene. It is noteworthy that a patient with relatively mild nonprogressive hepatic form of GSD IV also had two missense mutations (Leu224Pro and Tyr329Ser).[14] In contrast, 2 patients with a severe hepatic or neuromuscular form of GSD IV had a translation-terminating mutation or a splicing mutation.[14] It seems possible that subtle alterations of the amino acid sequence at certain sites might cause APBD limited mainly to the central and peripheral nervous system or mild hepatic and neuromuscular forms of GSD IV, whereas translation-terminating or disruptive mutations may be involved in a multisystemic severe phenotype of GSD IV. Further studies of the GBE gene in more patients may help in understanding the genotype/phenotype correlation in GSD IV. The molecular basis of APBD with normal GBE activity in leukocytes and peripheral nerves also remains to be determined.

Note Added in Proof

Since submission of this manuscript Bruno and colleagues[15] described the identical heterozygous G-to-A

transition at codon 524 (Arg524Gln) in a patient with a combination of hepatic and muscular features of GSD IV. This further supports our hypothesis that this genomic region may be a mutation hotspot in GSD IV.

We thank Dr C. Kubisch for critical reading of the manuscript.

References

1. Robitaille Y, Carpenter S, Karpati G, DiMauro S. A distinct form of adult polyglucosan body disease with massive involvement of central and peripheral neuronal processes and astrocytes: a report of four cases and review of the occurrence of polyglucosan bodies in other conditions such as Lafora's disease and normal aging. Brain 1980;103:315–336
2. Gray F, Gherardi R, Marshall A, et al. Adult polyglucosan body disease. J Neuropathol Exp Neurol 1988;47:459–474
3. Boulan-Predseil P, Vital A, Brochet B, et al. Dementia of frontal lobe type due to adult polyglucosan body disease. J Neurol 1995;242:512–516
4. Karpati G, Carpenter S. The clinical spectrum of adult polyglucosan body disease. Neurology 1983;33(Suppl 2):246 (Abstract)
5. McDonald TD, Faust PL, Bruno C, et al. Polyglucosan body disease simulating amyotrophic lateral sclerosis. Neurology 1993;43:785–790
6. Lossos A, Meiner Z, Barash V, et al. Adult polyglucosan body disease in Ashkenazi Jewish patients carrying the $Tyr^{329}Ser$ mutations in the glycogen-branching enzyme gene. Ann Neurol 1998;44:867–872
7. Bruno C, Servidei S, Shanske S, et al. Glycogen branching enzyme deficiency in adult polyglucosan body disease. Ann Neurol 1993;33:88–93
8. Chen YT, Burchell A. Glycogen storage diseases. In: Scriver CR, Beaudet AL, Sly WS, Valle D, eds. The metabolic and molecular basis of inherited diseases, vol 1. 7th ed. New York: McGraw-Hill, 1995:935–965
9. DiMauro S, Tsujino S. Nonlysosomal glycogenoses. In: Engel AG, Franzini-Armstrong C, eds. Myology, vol 2. 2nd ed. New York: McGraw-Hill, 1994:1554–1576
10. Sindern E, Patzold T, Vorgerd M, et al. Adulte Polyglukosankörperkrankheit. Fallbeispiel mit überwiegender Beteiligung des zentralen und peripheren Nervensystems und Branchingenzymdefekt in Leukozyten. Nervenarzt 1999;70:745–749
11. Grehl T, Müller K, Vorgerd M, et al. Impaired aerobic glycolysis in muscle phosphofructokinase deficiency results in biphasic post exercise phosphocreatine recovery in ^{31}P-MRS. Neuromusc Disord 1998;8:480–488
12. Thon VJ, Vigneron-Lesens C, Marianne-Pepin T, et al. Coordinate regulation of glycogen metabolism in the yeast *Saccharomyces cerevisiae*. J Biol Chem 1992;267:15224–15228
13. Baba T, Kimura K, Mizuno K, et al. Sequence conservation of the catalytic regions of amylolytic enzymes in maize branching enzyme-I. Biochem Biophys Res Commun 1991;181:87–94
14. Bao Y, Kishani P, Wu JY, Chen YT. Hepatic and neuromuscular forms of glycogen storage disease type IV caused by mutations in the same glycogen-branching enzyme gene. J Clin Invest 1996;97:941–948
15. Bruno C, DiRocco M, Lambda LD. A novel missense mutation in the glycogen branching enzyme gene in a child with myopathy and hepatopathy. Neuromusc Dis 1999;9:403–407

Mental Retardation and Behavioral Problems as Presenting Signs of a Creatine Synthesis Defect

Marjo S. van der Knaap, MD, PhD,*
Nanda M. Verhoeven, PhD,†
Petra Maaswinkel-Mooij, MD,‡
Petra J. W. Pouwels, PhD,§ Wim Onkenhout, PhD,‡
Els A. J. Peeters, MD,‖
Sylvia Stöckler-Ipsiroglu, MD, PhD,¶
and Cornelius Jakobs, PhD†

Recently, 3 patients with a creatine synthesis defect have been described. They presented with developmental regression, extrapyramidal movement abnormalities, and intractable epilepsy, and they improved with treatment of creatine monohydrate. We report 2 unrelated boys with a creatine synthesis defect and nonspecific presenting signs of psychomotor retardation, behavioral problems, and, in 1, mild epilepsy. Metabolic urine screening revealed elevations in all metabolites, expressed as millimoles per mole of creatinine, which suggests decreased creatinine excretion. This finding led to the correct diagnosis. We propose to include the assessment of the overall concentrations of amino acids and organic acids relative to creatinine in routine metabolic urine screening.

van der Knaap MS, Verhoeven NM, Maaswinkel-Mooij P, Pouwels PJW, Onkenhout W, Peeters EAJ, Stöckler-Ipsiroglu S, Jakobs C. Mental retardation and behavioral problems as presenting signs of a creatine synthesis defect. Ann Neurol 2000;47:540–543

Recently, an inherited metabolic disorder, caused by a defect in the synthesis of creatine, has been discovered.[1] Creatine and creatine phosphate are essential for the storage and transmission of phosphate-bound energy in muscle and brain. They are catabolized to creatinine. For maintenance of the body pool, the daily urinary loss of creatinine must be replenished by en-

From the *Department of Child Neurology, †Metabolic Unit of the Department of Clinical Chemistry, and §Department of Clinical Physics and Informatics, Free University Hospital, Amsterdam; ‡Department of Pediatrics, Leiden University Medical Center, Leiden; and ‖Department of Child Neurology, Juliana Children's Hospital, The Hague, The Netherlands; and ¶Department of Pediatrics, University Hospital of Vienna, Vienna, Austria.

Received Sep 30, 1999, and in revised form Dec 2. Accepted for publication Dec 4, 1999.

Address correspondence to Dr van der Knaap, Department of Child Neurology, Free University Hospital, PO Box 7057, 1007 MB Amsterdam, The Netherlands.

dogenous synthesis and dietary intake. A deficiency of guanidinoacetate methyltransferase (GAMT) is the first inborn error of creatine synthesis reported in humans.[2] It results in depletion of body creatine and accumulation of guanidinoacetate. The urinary excretion of creatinine, which is directly proportional to the body creatine pool, is low in defects of creatine synthesis.

The only 3 patients described thus far presented with developmental delay followed by regression,[1,3,4] muscle hypotonia,[1] extrapyramidal movement abnormalities,[1,3] and intractable epilepsy.[3,4] The neurological problems were progressive.[1–4] Supplementation with creatine monohydrate led to considerable neurological improvement but not to normalization.[1–4]

Developmental regression, intractable epilepsy, and extrapyramidal movement disturbances are current indications to pursue a creatine synthesis defect. However, considering the small number of patients reported, the entire clinical spectrum and, with that, the range of indications for screening may not be known. We add 2 patients without any specific neurological findings to the spectrum.

Patient Reports

Patient 1 is a boy who presented at 2.5 years because of developmental delay. He could stand with support at 13 months, but at 2.5 years he could still only walk with support. He had no language skills, neither receptive nor expressive. His development was progressing slowly but steadily. Mild temporary regressions were noted during febrile illnesses. The parents of the patient were healthy and nonconsanguineous. There was a healthy sister.

Physical examination revealed normal height, weight, and head circumference; there were no abnormalities of the internal organs. His behavior was autistic. He did not make eye contact, whereas there was no evidence of decreased vision. He avoided interpersonal interaction. Neurological examination revealed no abnormalities apart from a generalized moderate hypotonia. Ophthalmological examination was normal.

A magnetic resonance imaging scan of the brain revealed mildly retarded myelination. Chromosomes were normal. DNA analysis revealed no evidence of fragile X syndrome. Blood ammonia was normal. Metabolic screening of a 24-hour-sample of urine revealed a generalized elevation of the concentrations of amino acids, organic acids, and uric acid. Because these concentrations are expressed as millimoles per mole of creatinine, a low creatinine excretion related to a creatine synthesis defect was considered. Serum creatinine concentration was normal (38 mmol/L; normal, 25–75 mmol/L).

Patient 2 is a boy with developmental delay and mild hypotonia. Independent walking was achieved at 2 years. At 2.5 years, several epileptic seizures occurred during episodes of fever. With valproate therapy, he was seizure-free for 2 years; valproate was discontinued. At that time, his electroencephalogram showed no epileptic activity. At 5 years, he still had poor receptive and no expressive language skills. He was severely retarded mentally, hyperactive, and difficult to handle. The parents were nonconsanguineous. They had 2 other healthy children.

Physical examination revealed normal height, weight, and head circumference; there were no abnormalities of the internal organs. He displayed hyperactive behavior. Although he offered eye contact, interpersonal interaction was poor. Neurological examination revealed no abnormalities apart from minor hypotonia.

A magnetic resonance imaging scan of the brain was normal. Laboratory examinations revealed normal creatine kinase, lactate, pyruvate, and chromosomes. DNA analysis revealed no evidence of fragile X syndrome. Metabolic screening of a 24-hour sample of urine revealed a generalized elevation of the concentrations of amino acids, organic acids, sialic acid, and uric acid as expressed as millimoles per mole of creatinine. A creatine synthesis defect was considered. Serum creatinine concentration was low (25 and 15 mmol/L).

Materials and Methods

Magnetic resonance imaging and proton magnetic resonance spectroscopy (MRS) were performed at 1.5 T. Volumes of interest for MRS were selected in right parietal white matter (4 ml), basal ganglia (5 ml), and midparietal cortex (8 ml). In each volume of interest, two spectra were acquired—a fully relaxed, short-echo time STEAM (stimulated-echo acquisition mode) spectrum (repetition time/echo time/mixing time = 6,000/20/10 msec; 64 accumulations) and a PRESS (point resolved spectroscopy) spectrum with a longer echo time (repetition time/echo time = 3,000/135 msec; 64 accumulations). Metabolite concentrations were calculated from the STEAM spectra by using LCModel (S. W. Provencher, Uslar, Germany).[5,6] Metabolite concentrations are expressed as millimoles per liter of volume of interest. Data were compared with values obtained in age-matched healthy controls (n = 12; age, 2–5 years).[7]

MRS was performed during the diagnostic phase, and subsequently 1.5, 3, 6, and 12 months after initiation of treatment in Patient 1, and after 3 and 6 months in Patient 2.

Guanidinoacetate concentrations in body fluids were assessed by using stable isotope dilution gas chromatography/mass spectrometry.[8] Activity of GAMT was assessed in fibroblasts.[4,9] DNA analysis was performed by PCR amplification of exon 2 and sequence analysis of the amplification product.

Results

Clinical Follow-Up

Treatment with creatine monohydrate was started at a dosage of 500 mg/kg/day and increased to 600 mg/kg/day. Shortly before starting treatment, a febrile convulsion occurred in Patient 1. Subsequently, frequent minor seizures occurred, with staring and subtle myoclonus for a few seconds. Electroencephalography revealed multifocal epileptic activity. After 1 month of treatment with creatine monohydrate, the seizures stopped without the use of anti-epileptic drugs. He became less hypotonic and, within 1 month, he could walk without support. His autistic behavior improved. However, he was hyperactive and had a short attention span. Seizures

did not recur, but his electroencephalogram still showed multifocal epileptic activity. At 4 years, the boy has not developed any expressive language, but he understands simple sentences. After initiation of treatment, Patient 2 became more interactive and attentive. There was a temporary increase in hyperactivity, but in the course of 9 months his behavior normalized. He is now 6 years old and able to use single words.

Laboratory and Spectroscopy Results

Creatinine and guanidinoacetate concentrations in body fluids, and creatine concentrations in the brain, are presented in the Table. MRS results are illustrated in the Figure. MRS of the cortex, white matter, and basal ganglia revealed normal concentrations of *N*-acetylaspartate, choline, *myo*-inositol, glutamate, and glutamine, except for a decreased *N*-acetylaspartate concentration in the cortex of Patient 1 on all occasions (7.1 ± 0.4 mmol/L, compared with 8.2 ± 0.9 mmol/L in controls). The concentrations of guanidinoacetate in urine and plasma decreased under treatment but did not normalize. The concentrations of creatine in the brain increased but also did not normalize.

The diagnosis was confirmed in both patients by finding no detectable activity of GAMT in fibroblasts (<0.1 ng/mg of protein/hr; control range, 0.38–0.56 ng/mg of protein/hr). DNA analysis revealed homozygosity for 327 G-A mutation in Patient 1 and heterozygosity for the same mutation in his parents. DNA analysis of Patient 2 is in progress.

Discussion

Our patients differ from the reported patients with GAMT deficiency[1–4] in that they had a much milder presentation and lacked specific neurological findings. Their main problems consisted of a psychomotor retardation, developmental dysphasia, and behavioral problems. Both had mild epilepsy with a delayed onset. They showed improvement on initiation of treatment with creatine monohydrate, although, as in the patients described before,[1–4] they did not become normal. In Patient 1, there was a rapid improvement of motor skills after initiation of treatment. The behavior in both patients improved significantly, but they remained severely retarded mentally, with significant language problems.

The absence of complete recovery can be explained by irreversible damage acquired before treatment, the persistent elevation of guanidinoacetate, the failure of brain creatine concentrations to normalize, or, most likely, a combination of these. The first issue can be addressed by diagnosing and treating patients early. Guanidinoacetate is neurotoxic in high concentrations.[10] Further reduction of its concentration through competitive inhibition of arginine:glycine amidinotransferase by additional substitution of ornithine failed.[11] Cerebral creatine concentrations do not normalize,[12] even with higher creatine monohydrate dosages of 600 mg/kg/day. This can be ascribed to the fact that neurons lack an active high-capacity creatine transport/uptake system[13,14] and that part of cerebral creatine is probably synthesized locally.[15,16]

Considering that GAMT deficiency is at least a partially treatable condition, probably more so if the condition is detected early, screening of appropriate patients is important. Screening by determination of serum creatinine is not adequate, because the values can be within the normal range. Schulze and colleagues[3] recommended assessment of cerebrospinal fluid creatine and creatinine concentrations for screening purposes. The most reliable tests for screening are the estimation of guanidinoacetate in urine, plasma, or cerebrospinal fluid by gas chromatography/mass spectrometry,[8] and the assessment of cerebral creatine concentration by proton MRS.[1–4] In the presence of developmental regression, extrapyramidal movement abnormalities, and intractable epilepsy, these tests are justified. However, it seems hardly realistic to perform

Table. Laboratory and Spectroscopy Results

	Months after Treatment								
	Patient 1					Patient 2			
	0	1.5	3	6	12	0	3	6	Controls
Plasma creatinine (mmol/L)	38	47	49	52	56	15–25	57	58	25–75
Urine creatinine (μmol/kg/day)	25	23	60	70	45	26	—	—	88–132
Urine guanidinoacetate (mmol/mol of creatinine)	5,139	1,055	841	650	980	453–795	—	342	10–99
Plasma guanidinoacetate (μmol/L)	38.4	20.6	16.5	13.7	16.1	20.9–23.8	8.0	9.8	0.7–1.4
CSF guanidinoacetate (μmol/L)	13.7	—	—	—	—	15.2	—	—	0.046–0.182
Creatine white matter (mmol/L of VOI)	0.7	1.6	2.4	2.4	2.8	0.2	2.0	2.7	5.0 ± 0.4
Creatine cortex (mmol/L of VOI)	0.3	2.3	3.2	3.0	2.5	0.2	3.8	ND	6.4 ± 0.7
Creatine basal ganglia (mmol/L of VOI)	0.7	3.1	4.4	5.0	ND	1.0	4.9	ND	7.9 ± 0.6

CSF = cerebrospinal fluid; VOI = volume of interest; ND = not assessable ("not done") (because of serious movement artifacts).

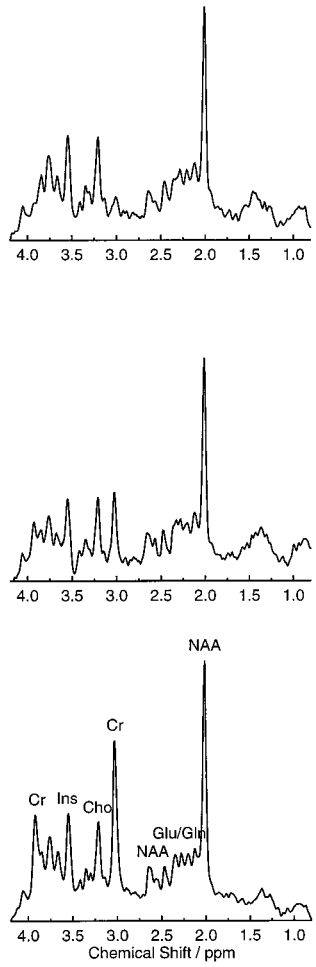

Fig. Magnetic resonance spectra of the parieto-occipital cortex in Patient 1 before treatment (top) and after 1 year of treatment with creatine monohydrate (middle), compared with a control spectrum (bottom). Note the almost complete absence of creatine (Cr) in the patient before treatment. With treatment, Cr increases but does not normalize. NAA = N*-acetylaspartate; Glu = glutamate; Gln = glutamine; Cho = choline-containing compounds; Cr = total creatine; Ins =* myo*-inositol.*

the tests in the numerous patients presenting with mental retardation, developmental dysphasia, and behavioral problems, with or without mild epilepsy. As a rule, "routine" metabolic urine screening will be performed in such cases. In both patients, we found a generalized increase in concentrations of all metabolites relative to creatinine, which led to the consideration of a creatine synthesis defect. Thus, we suggest that an assessment of the overall concentrations of amino acids and organic acids relative to creatinine should be included in the interpretation of routine metabolic urine screening results and that, in the case of a generalized increase, the possibility of a creatine synthesis defect should be investigated.

We thank Eduard A. Struys for the development of the stable isotope dilution gas chromatographic/mass spectrometric assay of guanidinoacetate and its application in the patients.

References

1. Stöckler S, Holzbach U, Hanefeld F, et al. Creatine deficiency in the brain: a new, treatable inborn error of metabolism. Pediatr Res 1994;36:409–413
2. Stöckler S, Isbrandt D, Hanefeld F, et al. Guanidinoacetate methyltransferase deficiency: the first inborn error of creatine metabolism in man. Am J Hum Genet 1996;58:914–922
3. Schulze A, Hess T, Wevers R, et al. Creatine deficiency syndrome caused by guanidinoacetate methyltransferase deficiency: diagnostic tools for a new inborn error of metabolism. J Pediatr 1997;131:626–631
4. Ganesan V, Johnson A, Connelly A, et al. Guanidinoacetate methyltransferase deficiency: new clinical features. Pediatr Neurol 1997;17:155–157
5. Provencher SW. Estimation of metabolite concentrations from localized in vivo proton MR spectra. Magn Reson Med 1993; 30:672–679
6. Pouwels PJW, Frahm J. Regional metabolite concentrations in human brain as determined by quantitative localized proton MRS. Magn Reson Med 1998;39:53–60
7. Pouwels PJW, Brockmann K, Kruse B, et al. Regional age dependence of human brain metabolites from infancy to adulthood as detected by quantitative localized proton MRS. Pediatr Res 1999;46:474–485
8. Struys EA, Jansen EEW, ten Brink HJ, et al. An accurate stable isotope dilution gas chromatographic-mass spectrometric approach to the diagnosis of guanidinoacetate methyltransferase deficiency. J Pharm Biomed Anal 1998;18:659–665
9. Ilias J, Mühl A, Stöckler-Ipsiroglu S. Guanidinoacetate methyltransferase (GAMT) deficiency: noninvasive enzymatic diagnosis of a newly recognized inborn error of metabolism. Clin Chim Acta (In press)
10. Hirayasu Y, Morimoto K, Otsuki S. Increase of methylguanidine and guanidinoacetic acid in the brain of amygdala kindled rats. Epilepsia 1991;32:761–766
11. Stöckler S, Marescau B, De Deyn PP, et al. Guanidino compounds in guanidinoacetate methyltransferase deficiency, a new inborn error of creatine synthesis. Metabolism 1997;46:1189–1193
12. Stöckler S, Hanefeld F, Frahm J. Creatine replacement therapy in guanidinoacetate methyltransferase deficiency, a novel inborn error of metabolism. Lancet 1996;348:789–790
13. Möller A, Hamprecht B. Creatine transport in cultured cells of rat and mouse brain. J Neurochem 1989;52:544–550
14. Tsuji M, Mulkern R, Cook C, et al. Relative phosphocreatine and nucleoside triphosphate concentrations in cerebral gray and white matter measured in vivo by ^{31}P nuclear magnetic resonance. Brain Res 1996;707:146–154
15. Holtzman D, Meyers R, O'Gorman E, et al. In vivo brain phosphocreatine and ATP regulation in mice fed with a creatine analogue. Am J Physiol 1997;272:C1567–C1577
16. Defalco AJ, Davies RK. The synthesis of creatine by the brain of the intact rat. J Neurochem 1961;7:308–312

Inclusion Body Myositis, Muscle Blood Vessel and Cardiac Amyloidosis, and Transthyretin Val122Ile Allele

Valerie Askanas, MD, PhD,* W. King Engel, MD,* Renate B. Alvarez, MSc,* Blas Frangione, MD, PhD,† Jorge Ghiso, PhD,† and Ruben Vidal, PhD†

Typical of sporadic inclusion body myositis muscle biopsies are vacuolated muscle fibers containing intracellular amyloid deposits and accumulations of "Alzheimer-characteristic" proteins. There is no muscle blood vessel or cardiac amyloidosis. We report on a 70-year-old African-American man homozygous for the transthyretin Val122Ile allele who has both sporadic inclusion body myositis and cardiac amyloidosis. His unique pathological features included transthyretin immunoreactivity in prominent muscle blood vessel amyloid and congophilic amyloid deposits within vacuolated muscle fibers.

Askanas V, Engel WK, Alvarez RB, Frangione B, Ghiso J, Vidal R. Inclusion body myositis, muscle blood vessel and cardiac amyloidosis, and transthyretin Val122Ile allele. Ann Neurol 2000;47:544–549

Sporadic inclusion body myositis (s-IBM), the most common acquired progressive muscle disease of older persons, is of unknown etiology and pathogenesis.[1,2] The most characteristic morphologic features of the s-IBM muscle biopsy are various degrees of lymphocytic inflammation, vacuolated muscle fibers, and Congo red–positive amyloid within muscle fibers.[1–3] The abnormalities within s-IBM muscle fibers have many similarities to those in the brain of Alzheimer's disease (AD) patients, including clusters of tau-containing paired helical filaments (PHFs), abnormal accumulations of β-amyloid protein (Aβ) and two other epitopes of β-amyloid precursor protein (AβPP),[4] apolipoprotein E (ApoE), several other "Alzheimer-characteristic" proteins, and markers of oxidative stress.[1,2]

Congophilic amyloid is not present in muscle blood vessels of s-IBM, and transthyretin (TTR) is not accumulated within s-IBM vacuolated muscle fibers or blood vessels[3] (Askanas, unpublished observation, February, 1998).

This report presents an African-American man with unusual muscle pathological features in association with s-IBM, which included TTR-immunoreactive amyloid in muscle blood vessels and intramuscularly. Because the patient also had amyloid cardiomyopathy identified by diphosphonate scan,[5] we asked the question whether the patient is positive for the TTR Val122Ile allele, the most common cause of late-onset cardiac amyloidosis among African Americans.[6] This study may serve as a background to generate hypotheses about the pathogenic relationship between types of amyloid and susceptibility to IBM.

Patient and Methods

Patient

A 70-year-old African-American man with type II diabetes has had progressive limb muscle weakness since November 1994, leading to severe disability. He also has had cardiomyopathy with congestive heart failure since 1993, his coronaries being angiographically normal. There was no family history of neuromuscular disease.

Neurological Examination

Neurological examination revealed the following: (1) pronounced weakness, slightly asymmetrical, of distal and proximal lower-limb muscles (MRC scale, where 5 is normal): iliopsoas 2, quadriceps 4, peronei 3, extensor hallucis longus 2, and flexor hallucis 2); (2) moderate proximal and distal weakness, slightly asymmetrical, of upper limb muscles: deltoid 3, biceps 4−, triceps 4, wrist flexors and extensors 4, flexor digitorum profundus 4−, extensor digitorum communis 4; (3) biceps tendon reflex reduced and all others absent; (4) no definite sensory loss.

Laboratory Studies

Blood studies showed creatine kinase (CK) to be 409 IU/L (normal, <161 IU/L) and CK-MB 5% (normal). No monoclonal gammopathy or increased immunoglobulins were found. Cerebrospinal fluid protein was 68 mg/100 ml (normal, <46 mg/100 ml), glucose was 72 mg/dl (normal), and IgG parameters were normal.

Diphosphonate Scan with Technetium 99m Hydroxyoliphosphonate

There was moderate diffuse uptake in the left ventricular myocardium. This is considered diagnostic of cardiac amyloidosis in the absence of hyperparathyroidism and recent massive myocardial infarction.[5]

From the *USC Neuromuscular Center, Department of Neurology, University of Southern California Keck School of Medicine, Good Samaritan Hospital, Los Angeles, CA; and †Department of Pathology, New York University School of Medicine, New York, NY.

Received Sep 8, 1999, and in revised form Oct 28 and Dec 9. Accepted for publication Dec 10, 1999.

Address correspondence to Dr Askanas, USC Neuromuscular Center, 637 South Lucas Avenue, Los Angeles, CA 90017-1912.

Electrophysiological Studies

Nerve conductions revealed low-amplitude motor and sensory responses with slowed conductions that were moderate to prominent and that had both axonal and demyelinating aspects. Electromyograms showed (1) a moderate number of fibrillations in 17 muscles of the upper and lower limbs; (2) long-duration high-amplitude polyphasic motor units predominately distally; and (3) BSAPPs (brief-duration, small-amplitude, overly abundant polyphasic motor-unit potentials) (indicating fractionation of motor units[7]), which were evident mainly proximally.

Left Biceps Muscle Biopsy

Ten-micron transverse sections of the fresh frozen biopsy were stained with 18 histochemical reactions and were used for immunocytochemistry as described.[4,8,9] Amyloid was evaluated with crystal-violet and the fluorescence-enhanced Congo red technique.[10]

Immunocytochemistry

The following antibodies were used against these antigens:

TTR: (1) rabbit polyclonal (Novocastra Laboratories, Inc, Vector, Burlingame, CA), diluted 1:20; and (2) goat polyclonal, peroxidase-conjugated and TRITC-conjugated (EY Laboratories, Inc, San Mateo, CA), both 1:100

AβPP epitopes: (1) rabbit polyclonal against Aβ 1-40 (from Dr D. Selkoe, Harvard Medical School, Boston, MA), 1:500; (2) mouse monoclonal 4G8 against Aβ17-24 (Senetek PLC, Napa, CA), 1:100; and (3) rabbit polyclonal against (a) AβPP C-epitope (from Dr S. Haga, Tokyo Institute of Psychiatry, Japan) and (b) AβPP N-terminal (from Dr B. Frangione, NYU Medical, New York, NY), both 1:500

ApoE: rabbit polyclonal (from Dr K. Weisgraber, University of California, San Francisco), 1:400

Phosphorylated tau: mouse monoclonals SMI-31 1:400 and SMI-310 1:200 (Sternberger Monoclonals, Inc, Baltimore, MD), recognizing phosphorylated tau on IBM PHFs[8]

Immunoglobulin light chains: (1) against lambda (a) mouse monoclonal, labeled with fluorescein isothiocynate (FITC; Kirkegaard and Perry Laboratories, Inc, Gaithersburg, MD), 1:5, and (b) goat polyclonal labeled with horseradish peroxidase (HRP; EY Laboratories), 1:10; (2) against kappa (a) mouse monoclonal, labeled with FITC (Kirkegaard and Perry), 1:5, and (b) goat polyclonal labeled with HRP (EY Laboratories), 1:10

To block nonspecific binding to Fc receptors, sections were preincubated with normal goat serum, diluted 1:10, as described.[4,8,9] Control was omitting the primary antibody or replacing the primary antibody with nonimmune rabbit serum or an irrelevant antibody.[4,8,9]

Electron Microscopy

Electron microscopy was performed on ultrathin sections of epon-embedded muscle. Gold and peroxidase immunoelectron microscopy were performed using 10-μm unfixed frozen transverse sections adhered to the bottom of a Petri dish, per our technique.[4,8,9]

Analysis of TTR *Gene*

Total genomic DNA was isolated from the patient's peripheral blood leukocytes. Polymerase chain reaction (PCR) using oligonucleotide flanking primers individually amplified the four *TTR*-coding exons.[11] The PCR products were visualized on ethidium-stained 5% polyacrylamide gels to confirm successful amplification, and the amplified DNA fragments were then subcloned into plasmid pCR2.1 (TA Cloning kit, Invitrogen Corp, Carlsbad, CA). Recombinant plasmid DNA was isolated for each exon and sequenced in both directions by the dideoxy chain termination method.

Results

Muscle Biopsy

Engel-Gomori trichrome staining[12] revealed typical features of s-IBM, including mononuclear cell inflammation and vacuolated muscle fibers (VMFs) (Fig 1A). Sixty to 70% of the VMFs contained congophilic deposits in the form of small intracellular plaques (see Fig 1F and G). VMFs also had accumulations of AβPP epitopes, including Aβ (Fig 2B).

Not seen in any other s-IBM patient were the following: (1) unique muscle blood vessel congophilia (see Fig 1B, D, and F) that was very strongly immunoreactive with all three TTR antibodies (see Fig 1C) and moderately immunoreactive with antibodies against Aβ (see Fig 1E); (2) strong TTR immunoreactivity within VMFs (see Fig 2A and C) co-localizing with AβPP, including Aβ (see Fig 2B), congophilic amyloid deposits (see Fig 2D), and ApoE. (ApoE is associated with congophilic amyloid in various types of amyloidosis.[13])

Only 20 to 30% of the VMFs contained SMI-31– and SMI-310–positive PHFs, compared with 70 to 80% of VMFs in typical s-IBM.[8]

Omitting the primary antibodies or their replacement with nonimmune sera gave negative results. Antibodies against immunoglobulin light chains did not react with any of the amyloid deposits.

Electron Microscopy

Electron microscopy revealed extracellular deposits of typical 6- to 8-nm amyloid-like fibrils within the blood vessel walls and outside some of the muscle fibers (see Fig 2E). Within the VMFs, there were intracellular deposits of the 6- to 8-nm fibrils and a variable number of lysosomal inclusions (see Fig 2F).

Immunoelectron Microscopy

TTR and Aβ antibodies immunodecorated 6- to 8-nm fibrils intracellularly within the VMFs and extracellularly in blood vessel walls (see Fig 2G–I). Rare SMI-31–positive PHFs were present within the VMFs. The

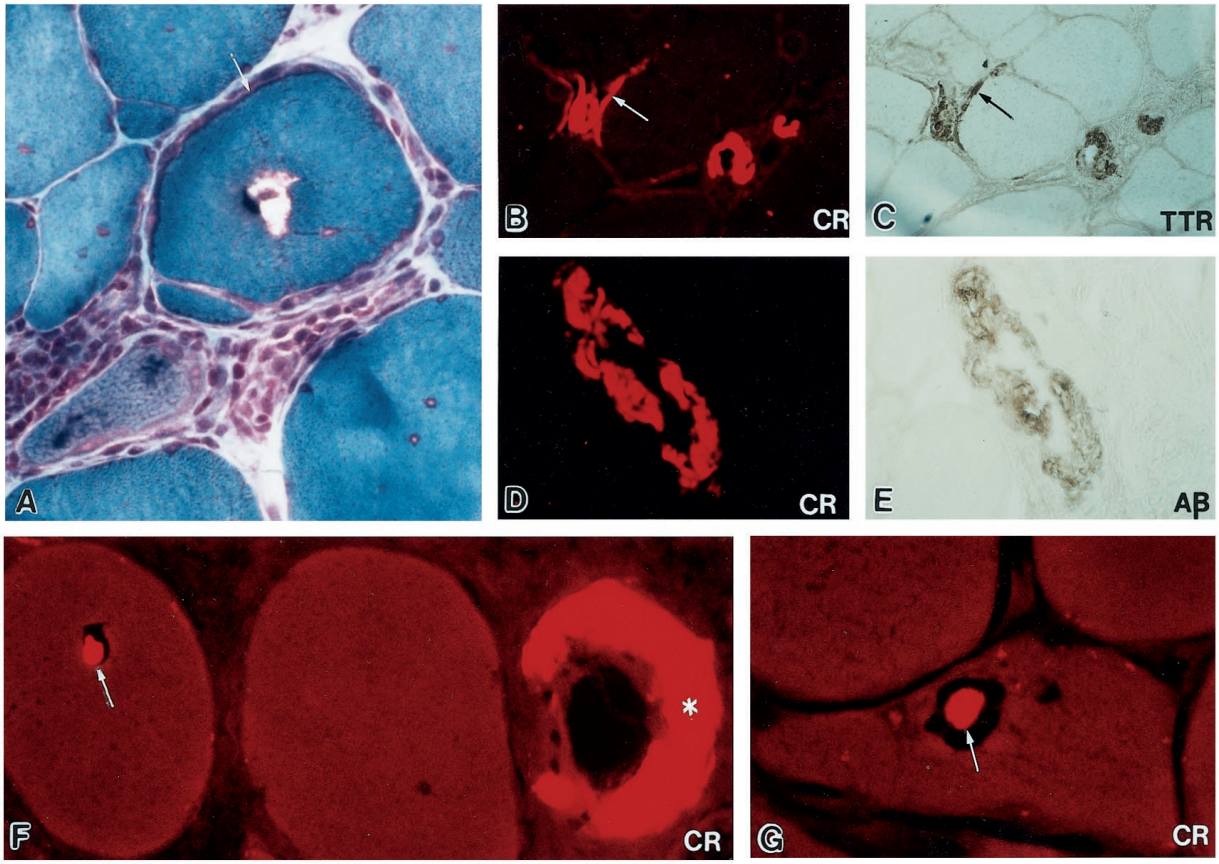

Fig 1. Light-microscopy of the patient's muscle biopsy. (A) Engel-Gomori trichrome staining showing vacuolated muscle fiber, (arrow) *and mononuclear cell inflammation. Colocalization of muscle blood vessel congophilia photographed through Texas red filters[10] (B and D) with immunoreactive TTR (C), and Aβ (E). In C, there is also TTR immunoreactivity colocalizing with congophilia (B) in a thin band at the periphery of the muscle fiber* (arrows). *(F and G) Congo red staining showing intracellular plaque-like amyloid deposits* (arrows), *and a prominent blood vessel congophilia* (* *in F*). *(Magnification: A, ×1,200; B–E, ×400; F and G, ×2,000).*

muscle biopsy morphological phenotypes of our patient and typical s-IBM are compared in the Table.

DNA Studies

We examined the entire coding sequence of the *TTR* gene after PCR amplification of the four exons. DNA sequencing analysis revealed a single change, A to G, in exon 4. That change in the first base of codon 122 resulted in the conversion of Val to Ile (Val122Ile). The patient was homozygous for the Val122Ile allele, as determined by DNA sequencing and restriction enzyme analysis with Tsp451 endonuclease.

Discussion

This is the first description of an association between s-IBM, cardiac amyloidosis, and the *TTR* gene mutation Val122Ile. Unique for s-IBM were TTR and Aβ immunoreactive muscle blood vessel amyloid, and TTR amyloid deposits within vacuolated muscle-fibers. Unusual for s-IBM were the intrafiber amyloid deposits' being virtually always in plaquette configuration rather than squiggles,[1,2] and a relative paucity of phosphorylated-tau–positive PHFs.

TTR is a 55-kd, 508–amino acid, tetrameric protein encoded by a gene on 18q12.1. It is involved in transport of thyroxin and retinol-loaded retinol-binding protein.[14,15] TTR constitutes the major amyloid protein in different forms of amyloidosis.[11,14,15] More than 60 distinct point mutations having been reported. TTR-derived amyloidosis is manifest usually as an autosomal dominant peripheral neuropathy or cardiomyopathy,[14,15] in which TTR amyloid is commonly deposited extracellularly in blood vessel walls and perimysium. In patients with the TTR Val122Ile mutation, TTR was identified in cardiac amyloid,[9] but Aβ was not sought. TTR amyloid was also found in blood vessels of some other organs, but muscle was not examined.[16] The TTR Val122Ile mutation has not yet been found in non–African Americans.[6,16]

In our patient, the following are possible:

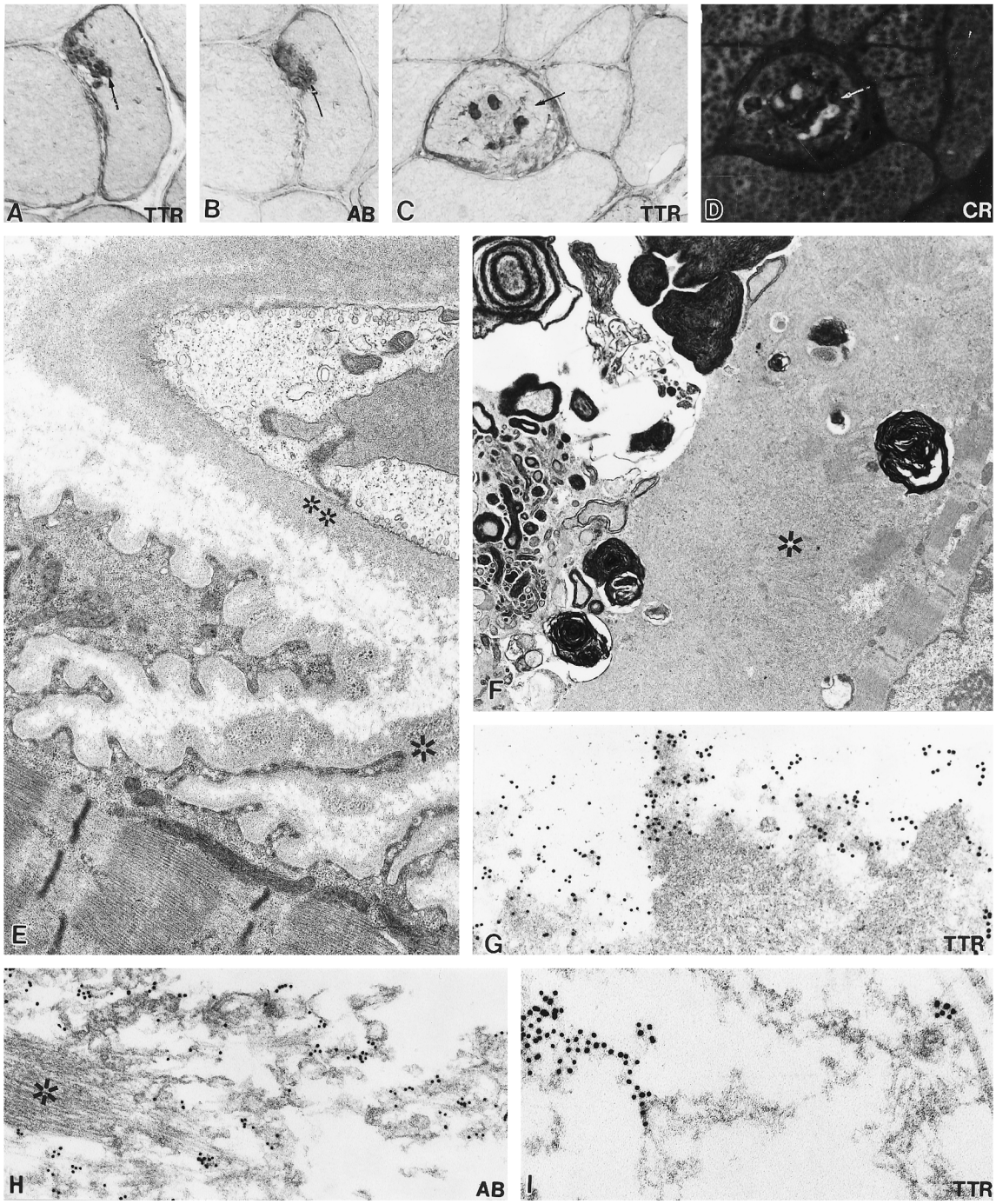

Fig 2. Light and electron microscopy. Darkly positive TTR (A) and Aβ (B) immunoreactive inclusions are seen in the same region of an abnormal muscle fiber on serial, but not adjacent, sections. TTR immunoreactive inclusions (C) and Congo red staining photographed through Texas red filters (D) on serial sections. Congo red positivity within the muscle fibers (arrow *in D*) *closely colocalizes with TTR immunopositivity* (arrow *in C*). *(E) Ultrastructural extracellular amyloid deposits outside the muscle fiber* (*) *and the blood vessels* (**). *(F) Vacuolated muscle fiber containing many dark osmiophilic intracellular lysosomal inclusions and a tightly packed amyloid inclusion* (*). *(G) Portion of a tightly packed amyloid deposit located within a muscle fiber is gold-immunolabeled with TTR, identified by the small dark gold particles. Positive immunoreactivity occurs only in the peripheral region of the deposit, where the amyloid fibrils are slightly dispersed, providing access to the antibody solution. (H) Within a muscle fiber, loosely packed amyloid deposits are immunolabeled with Aβ, whereas the adjacent portion of the myofiber* (*) *is not labeled. (I) Extracellular amyloid fibrils immunolabeled with TTR. Collagen fibril (right) is not labeled. (Magnification before 10% reduction: A–D, ×600; E, ×13,500; F, ×5,670; G and H, ×33,000; I, ×53,000. G–I, 10-nm gold particles.)*

Table. Comparison between IBM TTR Val122Ile and Typical s-IBM

	Our Patient IBM TTR Val122Ile[a]	Typical s-IBM
Muscle biopsy abnormalities		
Light microscopy		
Inflammation, mononuclear cells	+++	+ to +++
Vacuolated muscle fibers	+++	++ to +++
Transthyretin[b]		
In muscle fibers; small, plaque-like inclusions	+++	0
In muscle fibers; diffuse	++	0 to trace
In blood vessel walls	+++	0
Congophilia		
In muscle fibers; small, plaque-like inclusions	+++	++
In muscle fibers; squiggles	0 to +	+++
In blood vessel walls	+++	0
Amyloid β[b]		
In muscle fibers; small, plaque-like inclusions	+++	++
In blood-vessel walls; diffuse	++	0
Apolipoprotein E[b]		
In muscle fibers; small, plaque-like inclusions	+++	++
In muscle fibers; squiggles	0	+++
In blood vessel walls	++	0
Tau[b]		
SMI-31 and SMI-310 in muscle fibers; squiggles	+	+++
Electron microscopy		
Paired helical filament in muscle fibers	Rare	+++
6–10 nm amyloid filaments		
Muscle fibers, intracellular	+++	+ to ++
Blood vessels, extracellular	+++	0
Mitochondrial abnormalities	+ to ++	+ to ++
Cardiomyopathy		
Clinical criteria	++	0
Diphosphonate scan, heart amyloid	++	0

[a]Single change (A to G) in codon 122 (V 122 I); patient homozygous for the Val122Ile allele.

[b]Immunocytochemistry.

1. The TTR mutation made him susceptible to development of s-IBM or was the major cause of it. Although no other patients with TTR Val122Ile cardiac amyloidosis are known to have s-IBM–like muscle weakness, it might have been unrecognized or attributed to cardiac insufficiency.
2. There are two independent processes, (a) TTR Val122Ile mutant amyloid of heart and skeletal muscle blood vessels and (b) s-IBM, with possibly a partial influence of one or the other. In the blood vessels, the TTR amyloid probably provoked the Aβ accumulation, because in ordinary s-IBM, immunoreactive Aβ is not detectable there. Similarly, TTR Val122Ile might enhance the s-IBM–determined Aβ accumulation and fibrillogenesis within VMFs. The muscle fiber intracellular TTR accumulation probably was due to its being the Val122Ile mutant, because wild-type TTR does not accumulate within s-IBM fibers[3] (Askanas, unpublished observation, February, 1998). In our patient, the Val122Ile TTR may be bound to Aβ, since they colocalized. An aspect of the muscle fiber IBM milieu, such as Aβ accumulation, might have provoked the TTR Val122Ile accumulation there.

Experimental relationships of wild-type TTR and Aβ were described. In vitro, wild-type TTR can sequester Aβ and prevent amyloid formation.[17] In cultured vascular smooth muscle cells, wild-type TTR prevents intracellular accumulation of Aβ.[18] In AD patients, cerebrospinal fluid wild-type TTR is decreased[19] but of unknown significance. In general, perhaps wild-type TTR enhances Aβ catabolism while mutant TTR Val122Ile does not, thereby promoting Aβ amyloidogenesis.

In our patient, the TTR mutation has existed since conception, but both cardiomyopathy and IBM developed late in life, suggesting that aging of the cellular and extracellular milieu might be a contributing factor. Of interest is whether other elderly African-American patients with the Val122Ile allele and cardiac amyloidosis have IBM-like pathology or muscle blood vessel amyloid containing Aβ and TTR.

If the TTR Val122Ile allele is determined to be a susceptibility gene for s-IBM, other susceptibility genes should be sought.

This study was supported in part by NIH grants NS 34103 and AG 16768, and an MDA grant (all to V.A.). Work done in Dr Frangione's laboratory was supported by NIH grants AG 08721 and AG 05891.

We thank Drs Dennis Selkoe, T. Ishii, and S. Haga for antibodies against Aβ1-40 and C-terminal AβPP, and Dr Carl Weisgraber for antibody against ApoE.

References

1. Askanas V, Engel WK. Sporadic inclusion-body myositis and hereditary inclusion-body myopathies: current concepts of diagnosis and pathogenesis. Curr Opin Rheumatol 1998;10:530–542
2. Askanas V, Engel WK. Sporadic inclusion-body myositis and its similarities to Alzheimer disease brain: recent approaches to diagnosis and pathogenesis, and relation to aging. Scand J Rheumatol 1998;27:389–405
3. Mendell JR, Sahenk Z, Gales T, Paul L. Amyloid filaments in inclusion body myositis. Arch Neurol 1991;48:1229–1234
4. Askanas V, Alvarez RB, Engel WK. β-amyloid precursor epitopes in muscle fibers of inclusion-body myositis. Ann Neurol 1993;34:551–560
5. Kula RW, Engel WK, Line BR. Scanning for soft-tissue amyloid. Lancet 1977;1:92–93
6. Jacobson DR, Pastore RD, Yaghoubian R, et al. Variant-sequence transthyretin (isoleucine 122) in late-onset cardiac amyloidosis in black Americans. N Engl J Med 1997;336:446–473
7. Engel WK. Brief, small, abundant motor-unit action potentials. Neurology 1975;25:173–176
8. Askanas V, Engel WK, Yang C-C, et al. Light and electron microscopic immunolocalization of presenilin 1 in abnormal muscle fibers of patients with sporadic inclusion-body myositis and autosomal-recessive inclusion-body myopathy. Am J Pathol 1998;152:889–895
9. Askanas V, Engel WK, Alvarez RB. Enhanced detection of Congo-red–positive amyloid deposits in muscle fibers of inclusion-body myositis and brain of Alzheimer disease using fluorescence technique. Neurology 1993;43:1265–1267
10. Mirabella M, Alvarez RB, Bilak M, et al. Difference in expression of phosphorylated tau epitopes between sporadic inclusion-body myositis and hereditary inclusion-body myopathies. J Neuropathol Exp Neurol 1996;55:774–786
11. Vidal R, Garzuly F, Budka H, et al. Meningocerebrovascular amyloidosis associated with a novel transthyretin missense mutation at codon 18 (TTRD18G). Am J Pathol 1996;148:361–366
12. Engel WK, Cunningham GG. Rapid examination of muscle tissue: an improved trichrome method for fresh-frozen biopsy sections. Neurology 1963;13:919–923
13. Wisniewski T, Frangione B. Apolipoprotein E: a pathological chaperone protein in patients with cerebral and systemic amyloid. Neurosci Lett 1992;135:235–238
14. Benson MD. Leptomeningeal amyloid and variant transthyretins. Am J Pathol 1996;148:351–354
15. Saraiva MJM. Transthyretin mutations in health and disease. Hum Mutat 1995;5:191–196
16. Jacobson DR, Reveille JD, Buxbaum JN. Frequency and genetic background of the position 122 (Val → Ile) variant transthyretin gene in the black population. Am J Hum Genet 1991;49:192–198
17. Schwarzman AL, Gregori L, Vitek MP, et al. Transthyretin sequesters amyloid β protein and prevents amyloid formation. Proc Natl Acad Sci USA 1994;91:8368–8372
18. Mazur-Kolecka B, Frackowiak J, Wiśniewski HM. Apolipoproteins E3 and E4 induce, and transthyretin prevents accumulation of the Alzheimer's β-amyloid peptide in cultured vascular smooth muscle cells. Brain Res 1995;698:217–222
19. Serot J-M, Christmann D, Dubost T, Couturier M. Cerebrospinal fluid transthyretin: aging and late onset Alzheimer's disease. J Neurol Neurosurg Psychiatry 1997;63:506–508